Dimethyl Ether Synthesis from CO_2 and H_2 over Cu/ZnO-ZrO$_2$-Al$_2$O$_3$ and Zeolite

Miss Warangthat Kriprasertkul

จุฬาลงกรณ์มหาวิทยาลัย
CHULALONGKORN UNIVERSITY

A Thesis Submitted in Partial Fulfillment of the Requirements
for the Degree of Master of Engineering in Chemical Engineering
Department of Chemical Engineering
FACULTY OF ENGINEERING
Chulalongkorn University
Academic Year 2020
Copyright of Chulalongkorn University

การสังเคราะห์ไดเมทิลอีเทอร์จากคาร์บอนไดออกไซด์และไฮโดรเจนบนตัวเร่งปฏิกิริยาชนิด Cu/ZnO-ZrO_2-Al_2O_3 และซีโอไลต์

น.ส.วรางฑัต กรีประเสริฐกุล

วิทยานิพนธ์นี้เป็นส่วนหนึ่งของการศึกษาตามหลักสูตรปริญญาวิศวกรรมศาสตรมหาบัณฑิต
สาขาวิชาวิศวกรรมเคมี ภาควิชาวิศวกรรมเคมี
คณะวิศวกรรมศาสตร์ จุฬาลงกรณ์มหาวิทยาลัย
ปีการศึกษา 2563

Thesis Title	Dimethyl Ether Synthesis from CO_2 and H_2 over Cu/ZnO-ZrO_2-Al_2O_3 and Zeolite
By	Miss Warangthat Kriprasertkul
Field of Study	Chemical Engineering
Thesis Advisor	Assistant Professor Pattaraporn Kim, Ph.D.

Accepted by the FACULTY OF ENGINEERING, Chulalongkorn University in Partial Fulfillment of the Requirement for the Master of Engineering

.... Dean of the FACULTY OF ENGINEERING

(Professor SUPOT TEACHAVORASINSKUN, D.Eng.)
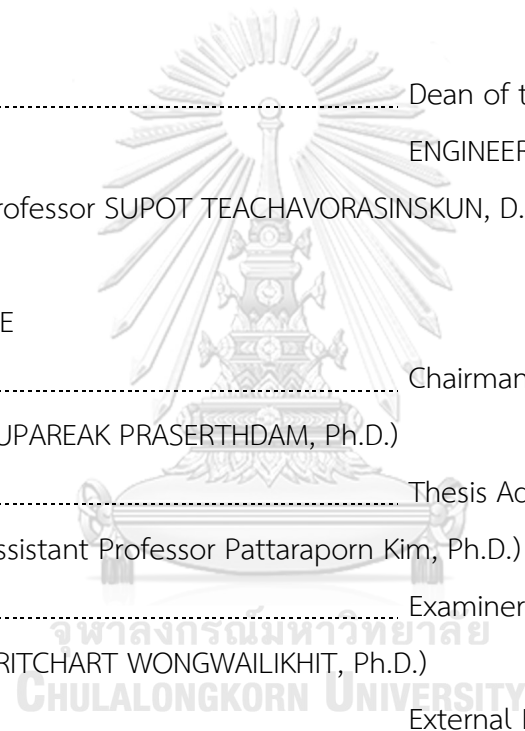
THESIS COMMITTEE

.... Chairman

(SUPAREAK PRASERTHDAM, Ph.D.)

.... Thesis Advisor

(Assistant Professor Pattaraporn Kim, Ph.D.)

.... Examiner

(KRITCHART WONGWAILIKHIT, Ph.D.)

.... External Examiner

(Associate Professor Thongthai Witoon, Ph.D.)

วรางฉัต กรีประเสริฐกุล : การสังเคราะห์ไดเมทิลอีเทอร์จากคาร์บอนไดออกไซด์และไฮโดรเจนบนตัวเร่งปฏิกิริยาชนิด $Cu/ZnO-ZrO_2-Al_2O_3$ และซีโอไลต์. (Dimethyl Ether Synthesis from CO_2 and H_2 over $Cu/ZnO-ZrO_2-Al_2O_3$ and Zeolite) อ.ที่ปรึกษาหลัก : ผศ. ดร.ภัทรพร คิม

ไดเมทิลอีเทอร์เป็นสารเคมีที่มีมูลค่าสูงชนิดหนึ่งที่ผลิตจากคาร์บอนไดออกไซด์ งานวิจัยนี้ได้ทำการสังเคราะห์ไดเมทิลอีเทอร์จากคาร์บอนไดออกไซด์ ซึ่งประกอบไปด้วย 2 ปฏิกิริยาหลัก ได้แก่ การสังเคราะห์เมทานอลจากคาร์บอนไดออกไซด์โดยปฏิกิริยาไฮโรจิเนชันด้วยวิธี ethanol-assisted และ การสังเคราะห์ไดเมทิลอีเทอร์จากเมทานอลโดยปฏิกิริยาดีไฮเดรชัน โดยมีการเติม ZrO_2, Al_2O_3 และ $ZrO_2-Al_2O_3$ ซึ่งใช้เป็นตัวส่งเสริม ปริมาณ 10% โดยมวล ลงในตัวเร่งปฏิกิริยาชนิด Cu/ZnO เพื่อเพิ่มประสิทธิภาพของตัวเร่งปฏิกิริยาในการสังเคราะห์เมทานอล และได้ทำการศึกษาเพื่อหาชนิดของซีโอไลต์ (ZSM-5 และ ferrierite) ที่เหมาะสมสำหรับปฏิกิริยาเมทานอลดีไฮเดรชัน จากนั้นศึกษาคุณลักษณะของตัวเร่งปฏิกิริยาชนิดต่างๆ ด้วยเทคนิค TGA, SEM-EDX, H_2-TPR, NH_3-TPD, BET และ XRD จากผลการทดลองพบว่าตัวเร่งปฏิกิริยาชนิด $Cu/ZnO/ZrO_2$ ทำให้ค่าการเปลี่ยนแปลงของคาร์บอนไดออกไซด์ และร้อยละผลได้ของเมทานอลสูงที่สุดถึง 82.1% และ 60% ตามลำดับ เนื่องจาก ZrO_2 มีส่วนช่วยให้ ขนาดผลึกของ CuO เล็กลง และพื้นที่ผิวสัมผัสของตัวเร่งปฏิกิริยาสูงขึ้น สำหรับการสังเคราะห์ไดเมทิลอีเทอร์จากเมทานอลโดยปฏิกิริยาดีไฮเดรชันพบว่า ferrierite มีความเป็นกรดสูงที่สุด ส่งผลให้ค่าการเปลี่ยนแปลงของเมทานอล และร้อยละผลได้ของไดเมทิลอีเทอร์สูงที่สุดถึง 47.09% และ 2.69% ตามลำดับ โดยการทดลองที่ใช้ตัวเร่งปฏิกิริยา $Cu/ZnO/ZrO_2$ และ ferrierite ทำให้เกิดไดเมทิลอีเทอร์สูงที่สุดถึง 0.4385 $mmol_{DME}/g_{cat}$ นอกจากนี้ยังพบว่ามีเอทิลีนซึ่งเป็นสารเคมีที่มีมูลค่าเกิดขึ้นจากการที่เอทานอลเกิดปฏิกิริยาดีไฮเดรชันที่สภาวะนี้ โดยได้ร้อยละผลได้ของเอทิลีนเท่ากับ 1.33% หรือ 5.45 $mmol_{Ethylene}/g_{cat}$

สาขาวิชา	วิศวกรรมเคมี	ลายมือชื่อนิสิต ....
ปีการศึกษา	2563	ลายมือชื่อ อ.ที่ปรึกษาหลัก ....

6270251021 : MAJOR CHEMICAL ENGINEERING

KEYWORD: CO2 conversion, Methanol, Dimethyl ether, Ethylene, Cu/ZnO-ZrO2-Al2O3, ZSM-5, Ferrierite

Warangthat Kriprasertkul : Dimethyl Ether Synthesis from CO_2 and H_2 over Cu/ZnO-ZrO_2-Al_2O_3 and Zeolite. Advisor: Asst. Prof. Pattaraporn Kim, Ph.D.

Dimethyl ether (DME) is one of higher-valued product from CO_2 conversion. In this study, the two steps of DME synthesis from CO_2 in a batch reactor, including CO_2 hydrogenation to methanol through ethanol-assisted method and methanol dehydration to DME, were investigated. The addition of 10 wt.% ZrO_2, Al_2O_3 and ZrO_2-Al_2O_3 as a promoter into Cu/ZnO was investigated to enhance the catalytic performance in methanol synthesis. Suitable types of zeolite (ZSM-5 and ferrierite) for methanol dehydration reaction were also determined. The catalysts were characterized by TGA, SEM-EDX, H_2-TPR, NH_3-TPD, BET and XRD. For the ethanol-assisted methanol synthesis, the Cu/ZnO/ZrO_2 catalyst provided the highest CO_2 conversion and methanol yield of 82.1% and 60.8%, respectively, since the addition of ZrO_2 decreased CuO crystallites size and increased surface area of catalyst. For methanol dehydration to DME, ferrierite provided relatively highest methanol conversion (47.09%) and DME yield (2.69%) due to its strongest acidity. The system with Cu/ZnO/ZrO_2 and ferrierite provided the highest DME productivity at 0.4385 $mmol_{DME}/g_{cat}$. Furthermore, under this conditions ethylene was produced as a valued by product of 1.33% yield or 5.45 $mmol_{Ethylene}/g_{cat}$ from dehydration of ethanol.

Field of Study:	Chemical Engineering	Student's Signature	....
Academic Year:	2020	Advisor's Signature	....

ACKNOWLEDGEMENTS

Warangthat Kriprasertkul

จุฬาลงกรณ์มหาวิทยาลัย
CHULALONGKORN UNIVERSITY

TABLE OF CONTENTS

LIST OF TABLES

LIST OF FIGURES

Chapter 1

Introduction

1.1 Motivation

Constantly increasing of atmospheric carbon dioxide (CO_2) due to human activities, for instance; burning fossil fuel especially coal, oil and natural gas in order to produces energy for transportation and industry, as a result of greenhouse effect. CO_2 is one of greenhouse gases. It trapped some of heat in the earth's surface to prevent reflection of heat to space. Thus, increasing of greenhouse gases produce higher cumulative heat of the Earth's surface called 'Global warming' [1].

The Mauna Loa Observatory (MLO), the US National Oceanographic and Atmospheric Administration (NOAA)'s Global Monitoring Laboratory (GML), revealed that atmospheric CO_2 measured of 417.1 ppm in May 2020, the highest ever measured. This year's value was higher than the last year in the same month of 2.4 ppm. In addition, the atmosphere CO_2 recorded at MLO from year 1958 to 2020 in Figure 1 shown the amount of CO_2 was increased and tend to constantly rise [2].
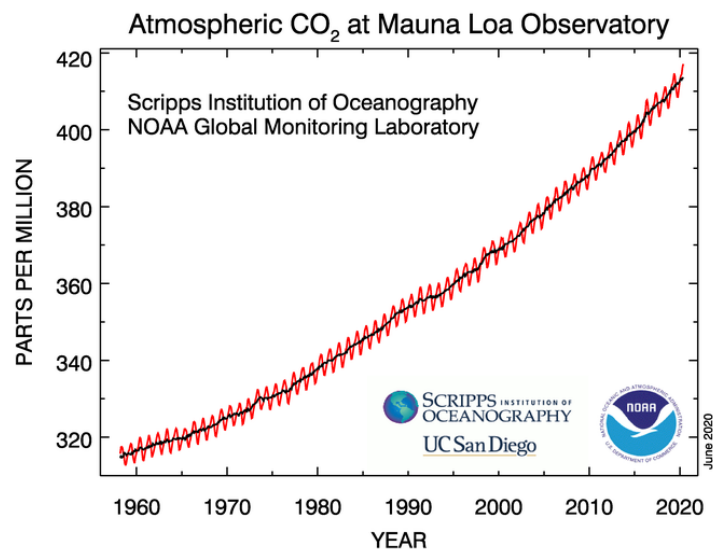
Figure 1 The atmosphere CO_2 recorded at MLO from year 1958 to 2020 [2]

The increasing Earth's surface temperature, caused greenhouse gases, as a result of melting glaciers and sea level rising might lead to disappearance region of

planet and other problems. That's not only has an impact on human but also impact on wildlife. They might lost their home or harder to find their food [3].

Therefore, reduction of CO_2 emission by utilization of CO_2 has increasing attention over the years. The utilization of CO_2 was classified into 2 categories including direct CO_2 utilization and CO_2 conversion to higher valued chemicals or fuels [4]. In this research, CO_2 was convert to dimethyl ether (DME), which is a promising alternative fuel because it is high efficiency in combustion at high cetane number. It is easy to transport and is clean fuel; low emission of NO_x and CO, sulfur-free and no soot when burn [5]. It can be applied in various segments such LPG blending, transportation fuel, chemical precursor for industries, etc.

The DME synthesis from CO_2 consists of 2 main reactions, methanol is firstly produced from CO_2 via hydrogenation reaction with Cu-based catalyst then the methanol dehydration reaction occurs over a solid-acid catalyst in the second step. Therefore, improving the catalytic performance of both reactions is considered to enhance productivity of DME.

In this research, ethanol-assisted method was used to synthesize methanol at lower temperature. Addition of promoter as ZrO_2, Al_2O_3 and ZrO_2-Al_2O_3 into Cu/ZnO prepared by co-precipitation method was investigated to enhance the catalytic performance in methanol synthesis. Suitable types of zeolite, including HZSM-5 (SAR=23 and 40) and ferrierite (SAR=18) was compared for methanol dehydration to DME. Two-step DME synthesis including ethanol-assisted methanol synthesis and methanol dehydration was carried-out in pressurized batch reactor.

1.2 Research objective

To synthesize dimethyl ether from CO_2 and H_2 over Cu/ZnO-ZrO_2-Al_2O_3 and zeolite and study optimal operating condition of reaction.

1.3 Research scopes

1.3.1 Methanol was produced from CO_2 and H_2 using a Cu/ZnO catalyst and the effect of ZrO_2, Al_2O_3 and ZrO_2-Al_2O_3 as a promoter was investigated.

1.3.2 Ethanol-assisted method was used to decrease operating temperature at 150°C and 50 bar of methanol production.

1.3.3 Cu/ZnO-based catalyst was synthesized by co-precipitation method with precipitation temperature of 65°C and constant pH value of 8 using Na_2CO_3 as precipitating agent.

1.3.4 DME was synthesized from methanol dehydration reaction with zeolite catalysts as ZSM-5 (SiO_2/Al_2O_3 molar ratios of 23 and 40) and ferrierite (SiO_2/Al_2O_3 molar ratios of 18).

1.3.5 Optimal operating condition of reaction was investigated.

1.3.6 TGA, XRD, SEM-EDX, BET surface areas, H_2-TPR and NH_3-TPD techniques were characterized catalysts.

1.3.7 Products were identified by using gas chromatography (GC) equipment to calculate conversion and yield.

1.4 Expected benefits

1.4.1 Reduce CO_2 emission by CO_2 conversion to highly value chemical as DME.

1.4.2 Enhance catalytic performance of DME synthesis process.

จุฬาลงกรณ์มหาวิทยาลัย

CHULALONGKORN UNIVERSITY

Chapter 2
Theory and Literature review

2.1 Dimethyl ether (DME)

Dimethyl ether (DME) or Methoxymethane is an ether in which the oxygen atom connected to two methyl groups (CH_3OCH_3). It is colorless gas with ether-like odor and noncorrosive. The chemical structure and physical properties are shown in Figure 2 and Table 1, respectively [6].
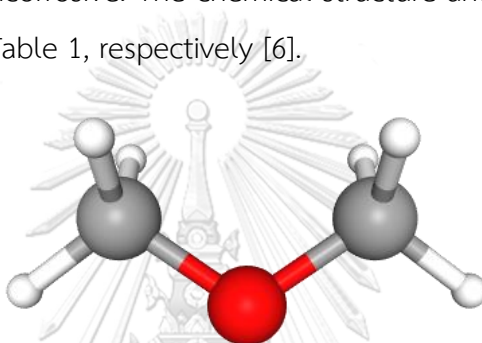
Figure 2 Chemical structure of DME [6]

Table 1 Physical properties of DME [6]

Property name	value	Unit
Molecular weight	46.07	g/mol
Density at -25°C	0.724	g/mL
Density at 25°C	1.9185	g/L
Melting point	-141.5	°C
Boiling point	-24.82	°C

In the past few year, DME has been used for alternative fuel, such as LPG blending, diesel replacement and gas turbine fuel, since it has high cetane number of 55 and be environmentally energy. It emits less NO_x, CO and particulate without sulfer compound. Furthermore, DME is easily transport because it's liquefied at moderate pressure.

Mordor Intelligence Organization [7] reported that in 2019, DME was the most commonly used as power generation followed by LPG blending, transportation fuel, aerosol products and other applications, respectively, as shown in Figure 3.

- ■ Aerosol Products
- ■ LPG Blending
- ■ Power Generation
- ■ Transportation Fuel
- ■ Other Applications
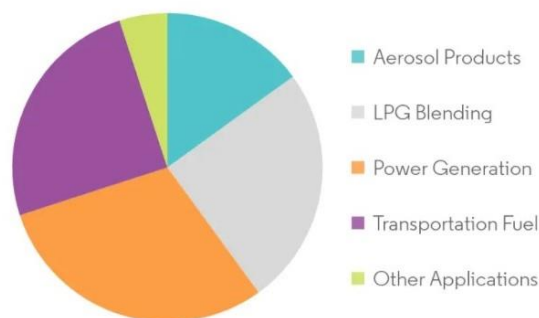
Figure 3 Global dimethyl ether market in 2019 [7]

2.2 DME synthesis from CO_2 and H_2

DME synthesis divides into indirect synthesis and direct synthesis.

2.2.1 The two-step process or indirect synthesis

Indirect DME synthesis, methanol is firstly produced from syngas or CO_2 via hydrogenation reaction (Eq. (1)) with Cu-based catalyst then methanol dehydration reaction occurred over solid-acid catalyst in the second reactor (Eq. (2)). The indirect DME synthesis process is shown in Figure 4.

$$CO_2 + 3H_2 \longleftrightarrow CH_3OH + H_2O \qquad \Delta H°_{298} = -49.4 \text{ kJ/mol} \qquad (1)$$

$$2CH_3OH \longleftrightarrow CH_3OCH_3 + H_2O \qquad \Delta H°_{298} = -23.4 \text{ kJ/mol} \qquad (2)$$
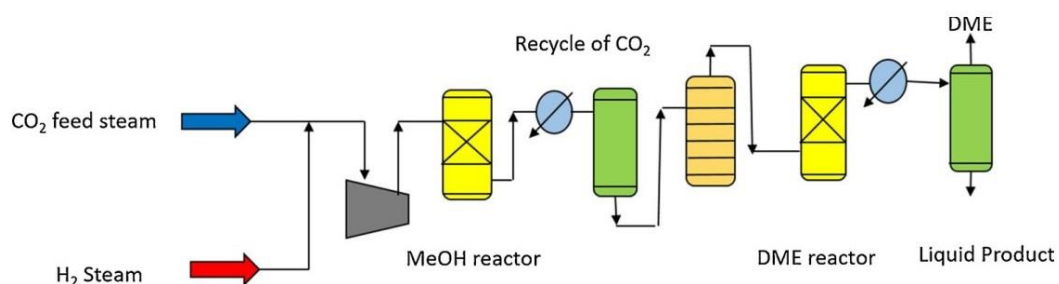
Figure 4 The two-step of DME production process from CO_2 and H_2 [8]

2.2.2 A single-step process or direct synthesis

A single-step DME production process is combination of hydrogenation, dehydration and the reverse water-gas shift reaction (rWGS) are presented in Eq. (1)-(3) with hybrid catalysts in one-pot. The overall reaction and DME production process from CO_2 and H_2 are exhibited in Eq. (4) and Figure 5, respectively.

$$CO_2 + H_2 \longleftrightarrow CO + H_2O \qquad \Delta H^{\circ}_{298} = 41.4 \text{ kJ/mol} \qquad (3)$$

$$2CO_2 + 6H_2 \longleftrightarrow CH_3OCH_3 + H_2O \qquad \Delta H^{\circ}_{298} = -122.2 \text{ kJ/mol} \qquad (4)$$
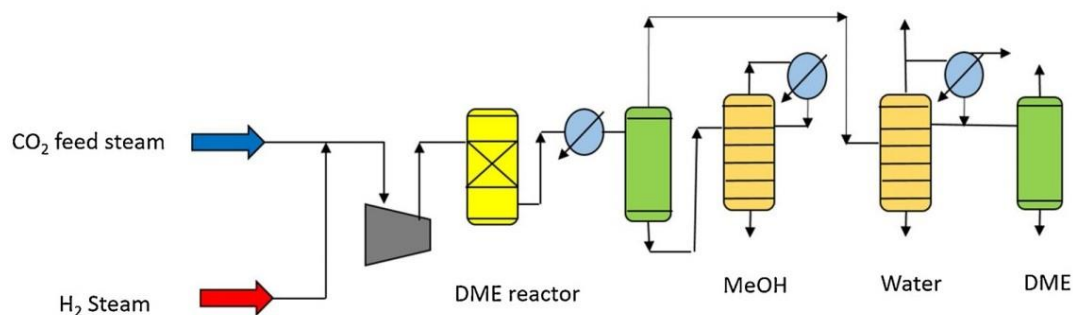
Figure 5 A single-step of DME synthesis process from CO_2 and H_2 [8]

The disadvantage of direct DME synthesis method is water formation during reaction, leading to the catalyst deactivation and decreasing yield of DME. However, the operational cost of direct DME synthesis method is less than indirect DME synthesis method.

Nakyai T. et al [9] was compared energy consumption and economic of indirect and direct DME synthesis from biomass. Process block flow diagrams of both method are illustrated in Figure 6 The result of simulation shows that the direct method consumed lower energy than indirect method about 28.73% that because indirect method requires the high energy for more reactors and distillations. Furthermore, comparison of the overall cost for both method indicated that the cost of indirect method is higher than direct method about 23.41%.
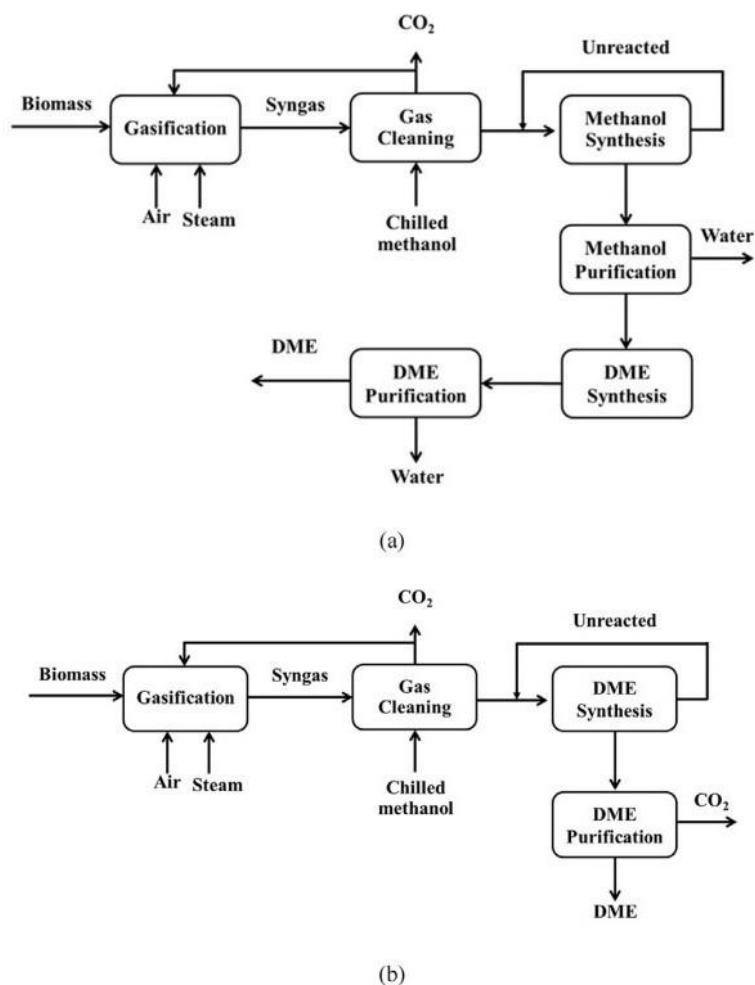
Figure 6 Block flow diagram of (a) indirect and (b) direct DME synthesis processes [9]

2.3 Catalysts for DME synthesis

The Cu-ZnO catalyst and solid-acid catalyst are the most commonly used for CO_2 hydrogenation and methanol dehydration to DME, respectively. Therefore, improving the catalytic performance of both reactions is considered to enhance yield of DME.

2.3.1 Methanol synthesis catalysts

To improve the catalytic performance of methanol synthesis reaction, many researchers have studied addition of various promoter such as TiO_2, ZrO_2, Al_2O_3, V_2O_5, etc. Various promoters have different functionalities. For example, the addition of zirconia (ZrO_2) leads to a decreasing in crystallite size of metallic and increases the

specific surface area causes increasing the Cu and ZnO dispersion as shown in the research of L'hospital V. et al. [10]. They studied the effect of ZrO_2 addition with different Zn/Zr ratio (Zn/Zr ratio = 100/0, 66/34, 50/50, 34/66 and 0/100) and kept the same Cu content of 30 %wt. The catalysts were prepared by conventional co-precipitation method. The reaction was carried out at pressure of 50 bar, various temperature between 240 and 300°C in a fixed-bed reactor. The results of catalytic characterization are shown in Table 2, presents the BET specific surface area increase when increasing ZrO_2 loading, $30Cu$-$ZZ_{0/100}$ is the highest. Moreover, the Cu surface area and Cu dispersion are the lowest when the support consisted of only ZnO or ZrO_2 although they has great in BET specific surface area. In contrast, when the support consisted both of ZnO and ZrO_2, the Cu surface area and Cu dispersion are greater, the $30Cu$-$ZZ_{50/50}$ catalyst has the highest Cu surface area and Cu dispersion.

Table 2 Characterization of the fresh 30Cu-ZnZr catalyst [10]

Catalyst	d_{app}[a]$(g\ cm^{-3})$	S_{BET}[b]$(m^2\ g^{-1})$	D (nm)[c]		CuO reducibility (%)[d]	S_{Cu}[e]$(m^2_{Cu}\ g_{cata}^{-1})$	D_{Cu} (%)	Content (wt%)[f]	
			CuO	ZnO				Cu	Na
30Cu-ZZ$_{100/0}$	0.32	41	12	13	91.2	6.4	3.3	31	0.01
30Cu-ZZ$_{66/34}$	0.51	79	10	10	95.1	10.5	5.4	30	_[g]
30Cu-ZZ$_{50/50}$	0.84	97	12	9	94.3	12.4	6.4	30	0.07
30Cu-ZZ$_{34/66}$	0.97	109	13	11	93.4	11.1	5.7	30	0.09
30Cu-ZZ$_{0/100}$	1.15	156	11	–	96.1	4.4	2.3	29	0.11
CuO		16							
ZnO		29							
ZrO$_2$		46							

[a] Apparent density.
[b] Specific surface area.
[c] Crystallite size determined by XRD using the Debye-Scherrer equation.
[d] CuO reducibility calculate from the amount of consumed H_2.
[e] Copper metallic surface area obtained by N_2O surface reaction.
[f] Content of each element determined by ICP-AES, the oxygen content wt% is not presented.
[g] Could not be determined due to technical limitations – very small quantity.

The catalytic test results are shown in Figure 7, presents that the $30Cu$-$ZZ_{66/34}$ catalyst at temperature of 260°C provides the highest methanol production of 453 $g_{MeOH}\ kg_{cat}^{-1}\ h^{-1}$. It is higher than $30Cu$-$ZZ_{100/0}$ which without ZrO_2 content of 75 $g_{MeOH}\ kg_{cat}^{-1}\ h^{-1}$ at the same temperature. Therefore, the addition of ZrO_2 leads to increasing the methanol productivity.
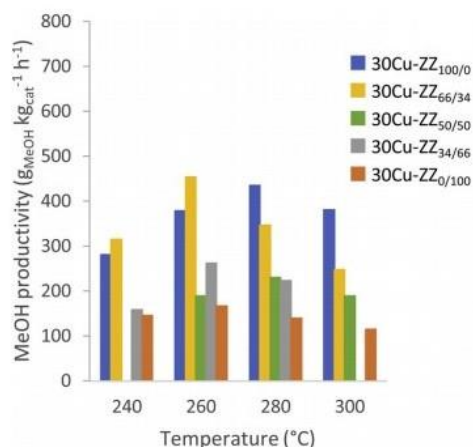
Figure 7 Methanol productivity at various temperatures [10]

Likewise, Xiao J. et al. [11] investigated effect of TiO_2, ZrO_2 and TiO_2-ZrO_2 promoted into Cu/ZnO catalyst with the ratio of Cu/ZnO/M was 40/40/20 when M substituted TiO_2, ZrO_2 and TiO_2-ZrO_2 via co-precipitation method.

The catalytic characterization results in XRD profiles of catalysts are shown in Figure 8, presents the intensity of peaks CuO and ZnO are less when TiO_2, ZrO_2 and TiO_2-ZrO_2 were added into catalysts. This indicated that TiO_2, ZrO_2 and TiO_2-ZrO_2 addition decrease crystallite size of CuO and ZnO which leads to increasing BET surface area and decreasing pore size of catalysts. The properties of various catalysts are shown in Table 3.
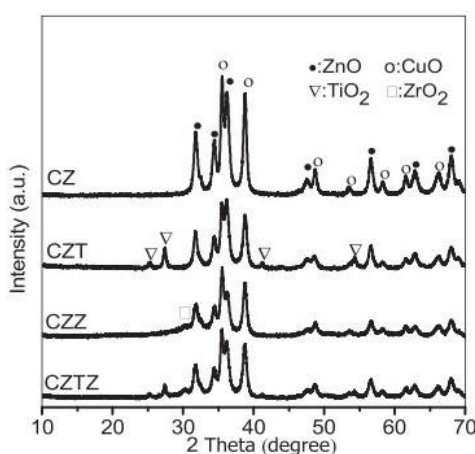
Figure 8 XRD profiles of various catalysts [11]

Table 3 The physicochemical properties of various catalysts [11]

Catalyst	S_{BET} (m²/g)	Pore size (nm)	Pore volume (cm³/g)	D^a_{CuO} (nm)	D^a_{ZnO} (nm)	S_{Cu} (m²/g)
CZ	26.3	27.7	0.18	18.9	15.1	4.89
CZT	37.3	22.2	0.21	16.4	14.9	5.17
CZZ	39.1	18.9	0.18	17.0	14.3	6.62
CZTZ	38.7	19.5	0.19	15.8	14.1	9.21

^{a} The crystallite size was estimated by Scherrer's equation.

The H_2-TPD analysis of catalysts revealed that the H_2 desorbed contents from active sites are shown in Table 4. The CZTZ catalyst provided the highest H_2 desorbed contents followed by CZZ, CZT and CZ, respectively. This related to Cu surface area as shown in Table 3.

Table 4 The H_2 and CO_2 adsorbed contents over various catalysts [11]

Catalyst	Amount of H_2 adsorbed		Amount of CO_2 adsorbed	
	A_α (a.u.)	A_β (a.u.)	A_α (a.u.)	A_β (a.u.)
CZ	7	256	15	19
CZT	33	305	37	9
CZZ	38	267	55	18
CZTZ	45	246	94	16

The CO_2-TPD curves of catalysts are shown in Figure 9, composes 2 peaks of weak basic site at lower temperature and strong basic site at higher temperature. It can be seen that the presence of TiO_2, ZrO_2 and TiO_2-ZrO_2 lead to increasing the amount of weak basic sites. Conclusion, the CZTZ catalyst is the highest Cu surface area and the amount of CO_2 adsorbed catalyst as shown in Table 4.
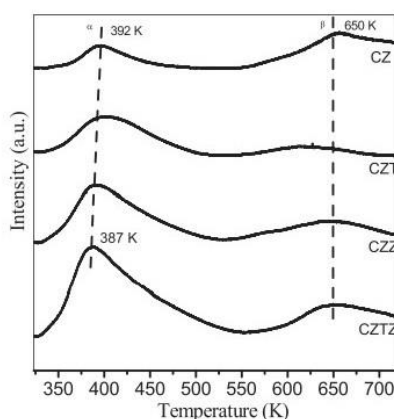
Figure 9 CO_2-TPD patterns of various catalysts [11]

The catalytic activity were investigated in fixed-bed reactor at temperature of 513 K and pressure of 3 MPa. The results are shown in Figure 10 indicated that the CO_2 conversion, methanol selectivity and methanol yield of catalysts which TiO_2, ZrO_2 and TiO_2-ZrO_2 were added, are higher than conventional Cu/ZnO catalyst. The CZTZ catalyst provides the highest percent methanol yield of 7.6%. This is correspond to the results of catalytic characterization.
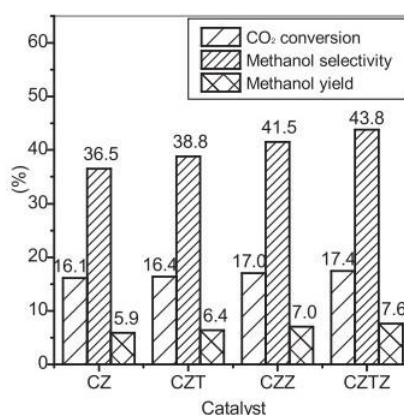
Figure 10 Effect of various promoters on catalytic performance [11]

For direct DME synthesis, $Cu/ZnO/Al_2O_3$ catalyst was used for methanol synthesis from CO_2 over the years. However, Al has the hydrophilic property, water generated in the reactions was adsorbed onto the catalyst. This leads to the catalyst deactivation and decreasing catalytic activity [12]. To improve this problem, the addition of promoter which has the hydrophobic property such as Zr was investigated including the research of Ren S. et al. [12].

Ren S. et al [12] modified a $Cu/ZnO/Al_2O_3$ by ZrO_2 (CZZA) and studied the activity and stability of catalysts. The catalysts was synthesized by co-precipitation method with atomic ratio of Cu/Zn/Zr/Al was 4:2:x:1 when x represents Zr loading varied from 0.5 to 1.5. The catalysts were mixed with HZSM-5 in 1:1 mass ratio and then tested in fixed-bed reactor at various temperature between 220 - 280°C with pressure of 2.76 MPa.

The catalytic characterization results revealed that CZZA with atomic ratio 4:2:1:0.5 provides the highest Cu surface area and Cu dispersion whereas the lowest Cu particle size. For this reason, CZZA with atomic ratio 4:2:1:0.5 is the best catalyst.

Furthermore, the addition of ZrO_2 decreased the Cu surface area but improved the Cu dispersion leading to a decrease Cu particle size.

The catalytic testing results are shown in Figure 11 indicated that the CZZA with 4:2:1:0.5 atomic ratio at reaction temperature of 240°C provided the highest CO_2 conversion and DME yield of 26.5% and 18.3%, respectively. In addition, Fig. 2.10 presents that the higher temperature lead to increasing CO production. Therefore, the reaction should be carried out in low temperature about 240°C.
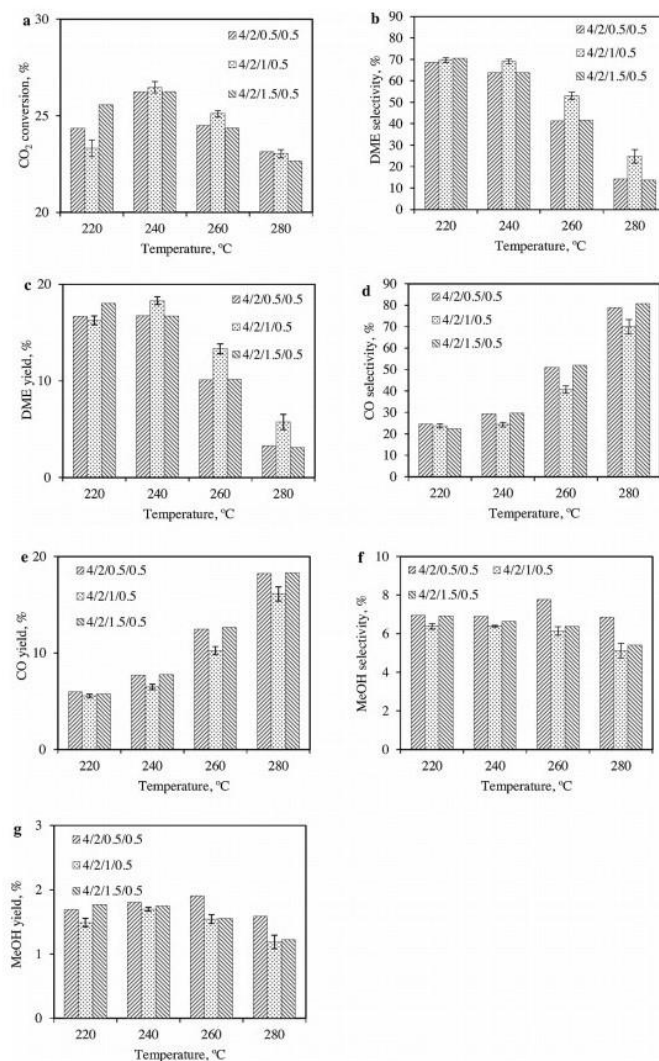
Figure 11 Effect of Zr loading in CZZA catalyst: (a) conversion of CO_2, (b) selectivity of DME, (c) yield of DME, (e) yield of CO, (f) selectivity of methanol, and (g) yield of methanol [12]

The stability of bifunctional catalysts were tested for 100 h. After 100 h, the results shows that the CO_2 conversion of CZZA/HZSM-5 catalyst is decreased from 27.1 to 24.1% while the CO_2 conversion of CZA/HZSM-5 (without Zr addition) catalyst is decreased from 26.2 to 22%. This indicated that the addition of ZrO_2 can improved the stability and activity of catalyst. The catalyst stability of CZZA and CZA mixed with HZSM-5 for DME synthesis are shown in Figure 12.
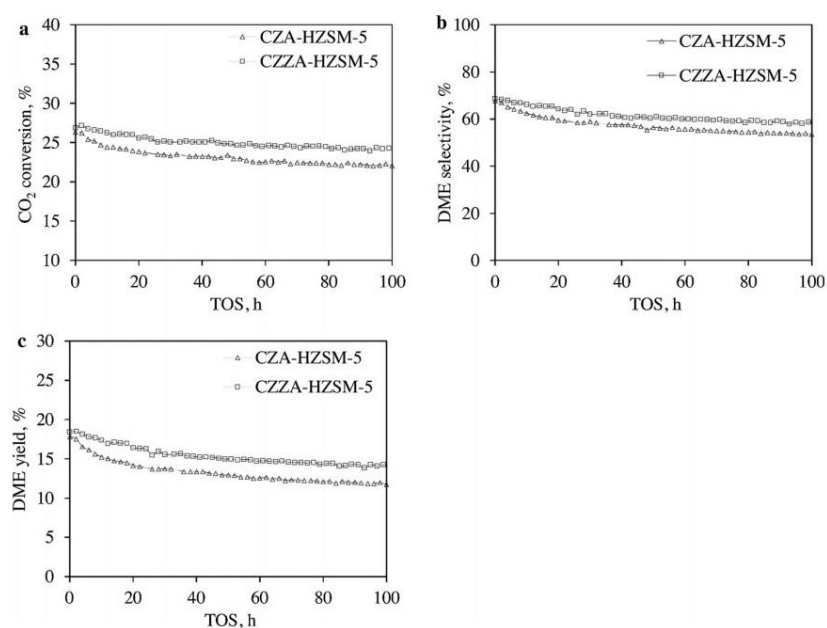
Figure 12 The catalyst stability of CZZA and CZA mixed with HZSM-5 for DME production: (a) conversion of CO_2, (b) selectivity of DME, and (c) yield of DME [12]

As the researches mentioned above implied that the presence of ZrO_2 enhances the performance and stability of catalyst for DME production. To further improve, Zhang Y. et al. [13] modified V_2O_5 onto $Cu/ZnO/ZrO_2$ as a quaternary catalysts. The $Cu/ZnO/ZrO_2/V_2O_5$ ($CZZV_x$) were synthesized by co-precipitation method with the mass ratio of $Cu/ZnO/ZrO_2/V_2O_5$ was 5:4:0.2:x when x represented V_2O_5 loading varied from 0 to 2 %wt. The $CZZV_x$ mixed with HZSM-5 as bifunctional catalysts ($CZZV_xH$). The reaction was tested in a fixed-bed reactor at 270°C and 3 MPa.

The results indicated that the addition of V_2O_5 leads to improve CO_2 conversion and DME yield. Since V_2O_5 addition enhance Cu dispersion, Cu surface area and BET surface area of catalysts. The CZZV$_{0.5}$H catalyst provides the highest conversion of CO_2 and yield of DME. The properties and the catalytic performance of catalysts are shown in Table 5

Table 5 The properties and the catalytic performances of catalysts [13]

Catalysts	S_{BET} (m²/g)	S_{Cu}[a] (m²/g)	d^b_{CuO} (nm)	d^c_{Cu} (nm)	Conversion Of CO_2 (%)	Selectivity (%)			DME yield (%)
						DME	CH$_3$OH	CO	
CZZV$_0$H	135.4	3.0	11.3	13.5	28.9	55.1	12.9	32.0	15.9
CZZV$_{0.25}$H	137.4	3.6	9.2	11.6	32.3	57.8	14.4	27.8	18.7
CZZV$_{0.5}$H	139.7	3.9	7.5	10.7	32.5	58.8	13.2	28.0	19.1
CZZV$_1$H	141.0	3.3	7.8	11.6	32.0	56.7	13.1	30.2	18.1
CZZV$_2$H	142.6	3.1	12.5	13.9	29.7	53.8	12.7	33.5	16.0

Reaction conditions: $T = 270$ °C; $P = 3.0$ MPa; CO_2:$H_2 = 1:3$; GHSV = 4200/h.
[a] Determined by nitrous oxide titration method.
[b] Diffraction spectra at $2\theta = 38.7°$ for CuO, and $31.7°$ for ZnO.
[c] Calculated from the surface area of metallic copper using a spherical particle model.

The NH$_3$-TPD curves of CZZV$_x$H catalysts are shown in Figure 13, display 3 desorption peaks in the temperature range of 100-200°C, 200-300°C and 300-400°C as weak, medium and strong acid site, respectively. It can see that the increasing V_2O_5 lead to the strength of acid site became stronger. The CZZV$_{0.5}$H catalyst is remarkably increases medium acid site and decreases strong acid site. This correspond to the most researches, implied that medium acid sites are more desirable for selectivity of DME while strong acid sites lead to by-products formation.
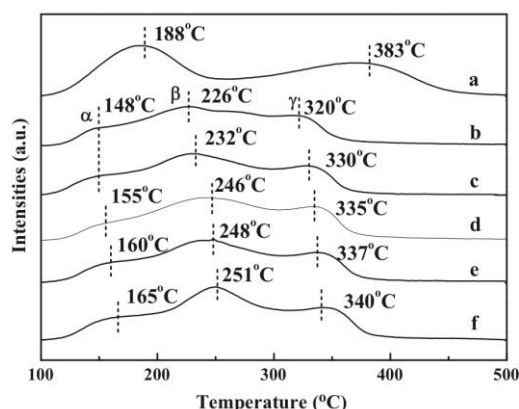
Figure 13 NH$_3$-TPD profiles of (a) HZSM-5, (b) CZZV$_0$H, (c) CZZV$_{0.25}$H, (d) CZZV$_{0.5}$H, (e) CZZV$_1$H and (f) CZZV$_2$H [13]

Besides the effect of promoter addition, the effect of catalytic preparation method was investigated. Sheng Q. et al. [14] studied the catalytic performance with various catalytic synthesis method as co-precipitation (C), sol-gel (S) and solid grinding (G). The $Cu/ZnO/ZrO_2$ and FER zeolite were used as hybrid catalyst with the atomic ratio of $Cu/ZnO/ZrO_2$ was fixed at 5:2:3. This hybrid catalysts represented CZZ(X)/FER, where X substituted the catalytic synthesis method.

The results of catalytic characterization by XRD technique are shown in Figure 14, exhibits the peaks of Cu, CuO, ZnO, ZrO_2 and FER in the hybrid catalysts. The peaks of Cu in CZZ(C)/FER catalyst in Figure 14(b) are broader than other catalysts. This indicated that the CZZ(C)/FER catalyst has smaller crystallite size. Hence, it is better dispersion and related to the crystallite sizes were calculated and shown in Table 6. The Cu crystallite sizes are decreases in order to CZZ(G)/FER, CZZ(S)/FER and CZZ(C)/FER, respectively.
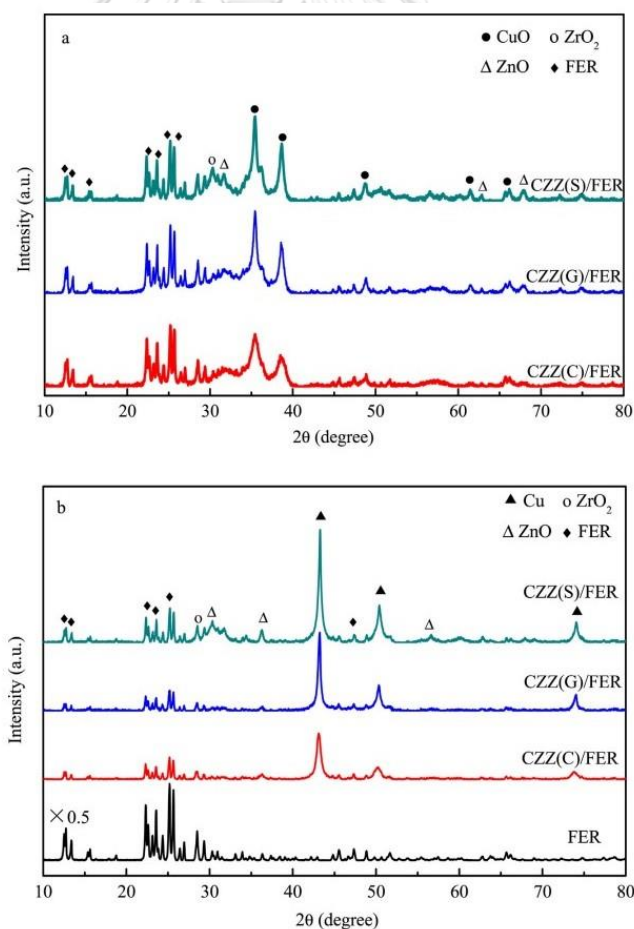
Figure 14 XRD curves of (a) the fresh and (b) reduced catalysts [14]

Table 6 The properties of the hybrid catalysts [14]

Catalyst	Surface area (m²/g)	Pore volume (cm³/g)	Average Pore diameter (nm)	CuO crystallite size (nm)	Cu crystallite size (nm)	ZnO crystallite size (nm)
CZZ(C)/ FER	245.1	0.42	6.9	10.9	17.5	18.6
CZZ(G)/ FER	230.1	0.26	4.5	14.3	29.1	27.0
CZZ(S)/ FER	222.5	0.27	4.9	14.7	28.3	28.2

Crystallite sizes were obtained using Scherrer's equation from the full width at half maximum (FWHM) data for the peaks at $2\theta = 35.5°$ for CuO, $43.3°$ for Cu, and $31.7°$ for ZnO.

The NH_3-TPD curves of catalysts are shown in Figure 15, composes 3 main peaks of weak, medium and strong acid sites in a temperature range of 100-300°C, 300-450°C and 450-650°C, respectively. The CZZ(C)/FER catalyst has the strongest of medium acid sites. Hence, CZZ(C)/FER is the best catalyst in terms of highest surface area, Cu dispersion and medium acid site contents.
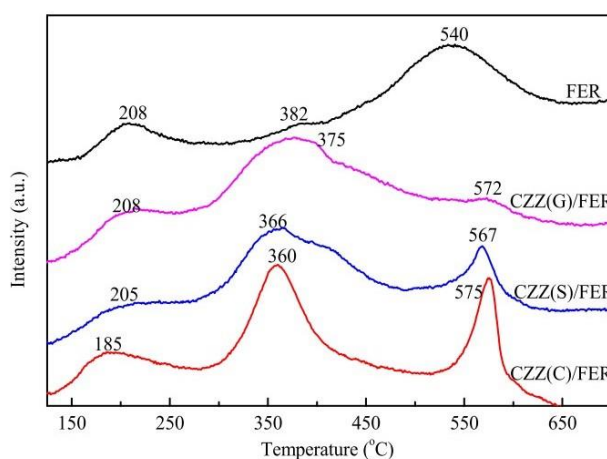
Figure 15 NH_3-TPD profiles of catalysts [14]

The catalysts were tested in a fixed-bed reactor with various temperature between 210 and 290°C and pressure of 2 MPa. The catalytic performance, including CO_2 conversion, DME selectivity, methanol selectivity, CO selectivity and DME yield are shown in Table 7. The results indicate that increasing temperature from 210 to 250°C, yield of DME increase for all catalysts. In contrast, after reaction temperature was increased higher 270°C, DME yield was decrease due to the rate of rWGS reaction is faster than methanol synthesis at high temperature. Therefore, the optimum reaction temperature is 250°C. At 250°C, the CZZ(C)/FER catalyst provides

the highest DME yield of 5% followed by CZZ(G)/FER and CZZ(S)/FER as 4.4% and 3.5%, respectively.

Table 7 Catalytic performance of hybrid catalysts [14]

Catalyst	T_R (°C)	X_{CO2} (%)	S_{DME} (%)	S_{CH3OH} (%)	S_{CO} (%)	Y_{DME} (%)
CZZ(C)/	210	10.8	25.7	14.5	59.8	2.8
FER	230	14.9	28.5	13.3	58.2	4.3
	250	17.5	28.4	13.3	58.3	5.0
	270	20.2	17.6	11.3	71.1	3.6
	290	23.5	7.0	9.4	83.6	1.6
CZZ(G)/	210	8.5	28.5	18.2	53.6	2.4
FER	230	13.9	25.6	13.6	50.8	3.6
	250	18.0	24.6	13.8	61.6	4.4
	270	21.1	17.1	13.0	69.9	3.8
	290	22.4	6.9	9.2	83.9	1.5
CZZ(S)/	210	6.5	32.3	21.8	45.9	2.1
FER	230	11.3	23.9	15.8	60.3	2.7
	250	17.4	20.3	13.5	66.2	3.5
	270	20.4	15.6	11.5	72.9	3.2
	290	21.5	6.6	10.6	82.8	1.4

Reaction conditions: T_R = 210−290°C, P_R = 2.0 MPa, GHSV = 1800 mL/(g_{cat}·hr). CZZ(C)/FER, CZZ(G)/FER, CZZ(S)/FER refer to Cu−ZnO−ZrO$_2$ supported on commercial ferrierite (FER) zeolites prepared by coprecipitation (C), citrate sol-gel (G), the solid grinding (S), respectively. T_R: reaction temperature; P_R: reaction pressure; GHSV: gaseous hourly space velocity; X_{CO2}: CO$_2$ conversion; S_{DME}: selectivity to DME; S_{CH3OH}: selectivity to methanol CH$_3$OH; S_{CO}: selectivity to CO; Y_{DME}: yield of DME.

2.3.2 Dehydration of methanol to DME catalysts

Usually, Al$_2$O$_3$ and various types of zeolites were used as a solid acid catalyst for dehydration reaction. There are many researches that studied various types of zeolites to find the best catalyst for this reaction, such as the researches are shown below.

To begin with Ramos et al.'s work [15], They compared the performance of solid acid catalysts as porous alumina (Al$_2$O$_3$-C), non-porous alumina (Al$_2$O$_3$-D), HZSM-5 (SiO$_2$/Al$_2$O$_3$ or SAR=40), sulfated-zirconia (S-ZrO$_2$) and tungsten-zirconia (W-ZrO$_2$) mixed with Cu/ZnO/Al$_2$O$_3$ catalyst (ACZ) for direct DME production from syngas.

The direct synthesis from syngas composed 3 main reactions as syngas hydrogenation to methanol (Eq. (5)), methanol dehydration (Eq. (2)) and the water-gas shift reaction (Eq. (6)).

$$CO + 2H_2 \longleftrightarrow CH_3OH \qquad \Delta H°_{298} = -90.6 \text{ kJ/mol} \qquad (5)$$

$$CO + H_2O \longleftrightarrow CO_2 + H_2 \qquad \Delta H°_{298} = -23.4 \text{ kJ/mol} \qquad (6)$$
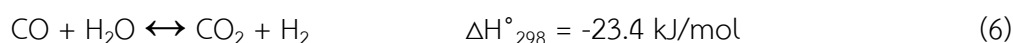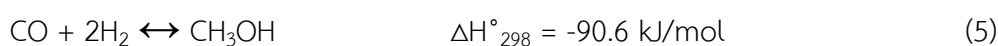
The BET surface area of solid acid catalysts of W-ZrO_2, Al_2O_3-D, S-ZrO_2, Al_2O_3-C and HZSM-5 are 94, 110, 143, 210 and 341 m^2/g, respectively. The pyridine adsorbed spectra on solid acid catalysts are shown in Figure 16, presents alumina samples adsorbed bands at 1450, 1490, 1575, 1595, 1613 and 1620 cm^{-1} (Figure 16(A)) indicated Lewis acid site. In contrast, the spectra of HZSM-5 and zirconia-based samples are shown in Figure 16(B), displays both of Lewis acid sites (1450, 1490 and 1610 cm^{-1}) and BrÖnsted acid site (1490, 1540 and 1640 cm^{-1}).
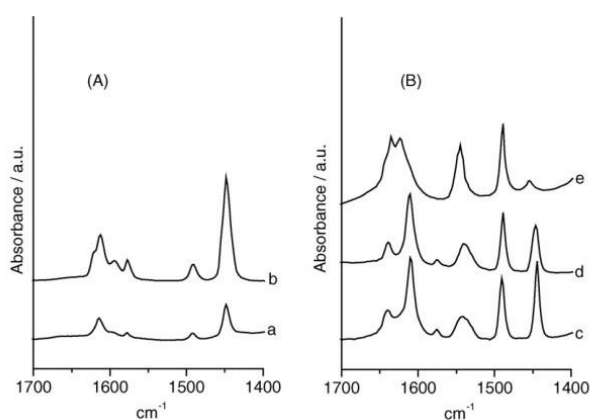
Figure 16 Infrared spectra of pyridine adsorption of (A) Al_2O_3-D (a), Al_2O_3-C (b); (B) S-ZrO_2 (c), W-ZrO_2 (d) and HZSM-5 (e) [15]

The acid strength of pyridine desorption temperature of solid acid catalysts are shown in Figure 17. For Lewis acid sites, Al_2O_3-C has higher amounts than Al_2O_3-D at low temperature while HZSM-5 and zirconium-based samples have the same pattern. For BrÖnsted acid site, HZSM-5 is significantly larger amounts than zirconium-based samples.
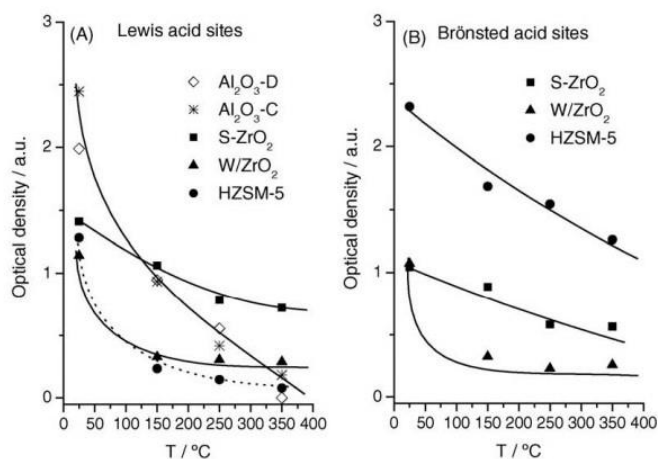
Figure 17 Acid strength of the pyridine adsorption temperature of various solid acid catalysts [15]

The results of catalytic testing in terms of CO consumption rate and selectivity are shown in Figure 18 and 19, respectively. The result shows that HZSM-5 and S-ZrO$_2$ have similar the highest CO consumption rate and selectivity of DME, followed by Al$_2$O$_3$-C, W-ZrO$_2$ and Al$_2$O$_3$-D, respectively. This imply that the catalysts which composed BrÖnsted acid sites has higher performance than the catalysts which composed only Lewis acid sites. Moreover, the stronger acid catalysts provide higher DME selectivity.
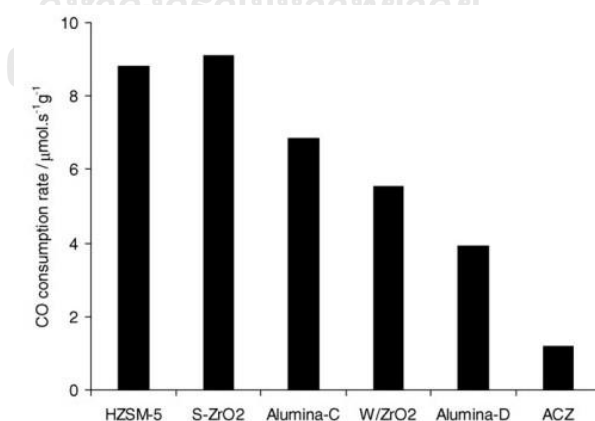
Figure 18 CO consumption rate of ACZ catalyst mixed with various solid acid catalysts [15]
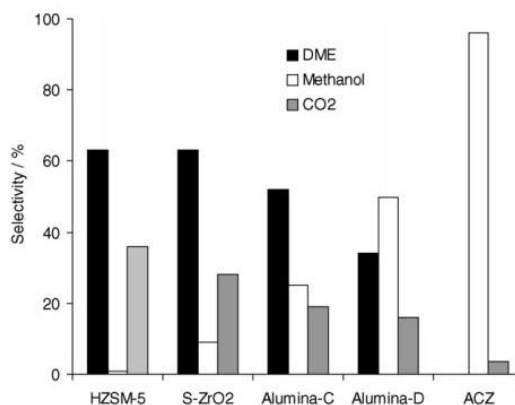
Figure 19 Selectivity of DME, methanol and CO_2 of the ACZ catalyst mixed with various solid acid catalysts [15]

Figure 19 exhibits the methanol selectivity of HZSM-5 catalysts has close to zero. This indicated that HZSM-5 which has the highest amounts of Brönsted acid sites, can improves rate of methanol dehydration reaction.

For another, Frusteri F. et al. [16] investigated the catalytic performance of $Cu/ZnO/ZrO_2$ in an atomic ratio of 60:30:10 with various types of zeolites as mordenite (MOR), ferrierite (FER) and HZSM-5 (MFI) for direct DME production from CO_2. Catalysts were synthesized by co-precipitation of the metallic in a solution of various zeolites. The mass ratio of $Cu/ZnO/ZrO_2$: zeolite was 2:1. The reaction was carried out at various temperature 200-260°C and 5 MPa in a fixed-bed reactor.

The results of N_2O chemisorption of the hybrid catalysts are shown in Table 8, reveals that the Cu crystallite size of CZZ-MOR, CZZ-FER and CZZ-MFI is 7.7, 8.4 and 9.4 nm, respectively. The metal surface area and metal dispersion are similar for all catalysts.

Table 8 Results of N_2O chemisorption of the hybrid catalysts [16]

Sample	MSA^a [m^2/g]	D_{Cu}^b [%]	d_{Cu}^c [nm]
CZZ-MOR	33	13.5	8
CZZ-FER	31	12.4	8
CZZ-MFI	27	11.1	9

[a] Copper surface area.
[b] Copper dispersion.
[c] Average copper particle size.

The SEM-EDX results are shown in Figure 20, presents large metal-oxide agglomerate on the zeolite matrix in CZZ-MOR and CZZ-MFI samples. In contrast, CZZ-FER sample presents good dispersion of metal-oxide on FER matrix.
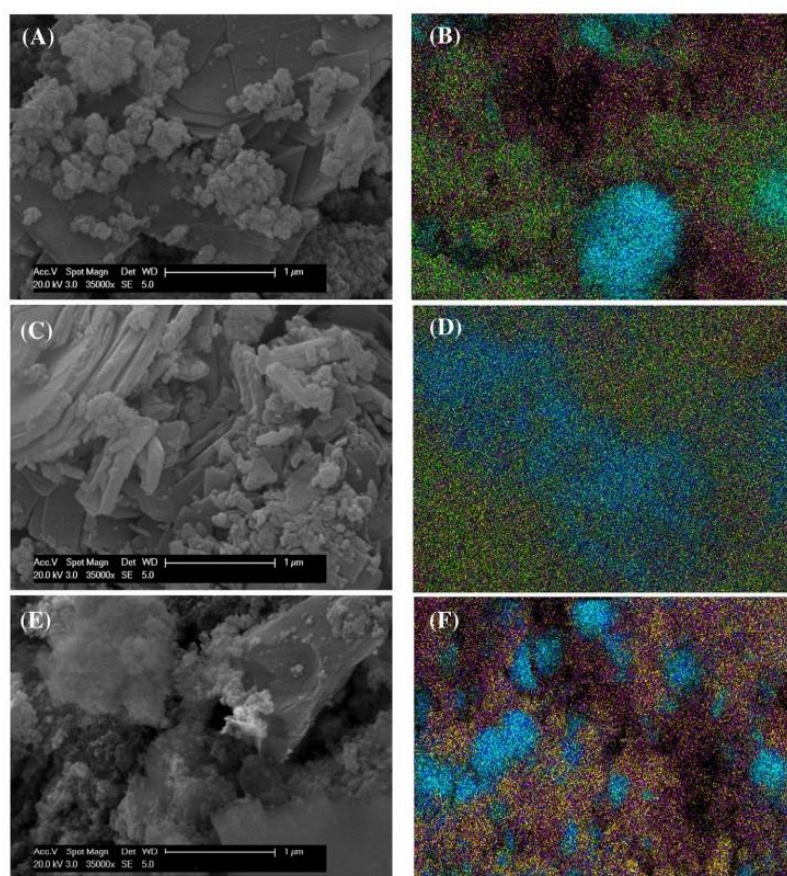
Figure 20 SEM-EDX images of (A-B) CZZ-MOR, (C-D) CZZ-FER and (E-F) CZZ-MFI [16]

The CO_2-TPD patterns of hybrid catalysts are shown in Figure 21(A), composes CO_2 desorption peaks at lower temperature (weakly basic sites) and higher temperature (strongly basic sites). CZZ-MOR and CZZ-MFI samples are mainly consist of weak basic sites, while CZZ-FER sample is consists of weak basic sites and strong acid sites with similar amounts. The results of TPD measurements of catalysts are shown in Table 9.

Also the NH_3-TPD profiles compose 2 main peaks of weak and strong acid sites. The quantitative data are shown in Table 9, indicated that the hybrid catalyst has significantly lower amounts of strong acid sites when compared with bare zeolites. However, CZZ-FER sample presents the highest acid capacity of 381 $\mu mol/g_{cat}$ with larger amounts both of weak and strong acid sites when compared with other hybrid catalysts.
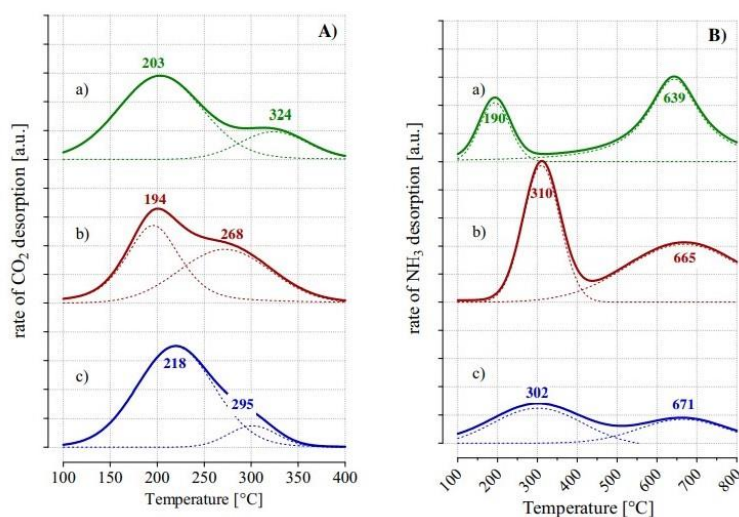
Figure 21 TPD profiles of (A) CO_2 and (B) NH_3: (a) CZZ-MOR; (b) CZZ-FER; (c) CZZ-MFI [16]

Table 9 Results of TPD measurement of the catalysts [16]

Sample	Base capacity[a] [$\mu mol/g_{cat}$]	Weak sites[b]	Strong sites[c]	Acid capacity[d] [$\mu mol/g_{cat}$]	Weak sites[e]	Strong sites[f]
CZZ-MOR	124	98	26	197	102	95
MOR				710	185	525
CZZ-FER	132	64	68	381	229	152
FER				653	235	418
CZZ-MFI	123	109	14	138	112	26
MFI				515	232	283

[a] Cumulative basicity in the range of 100–500 °C.
[b] Population of weak base sites between 100 and 250 °C.
[c] Population of strong base sites between 250 and 500 °C.
[d] Cumulative acidity in the range of 100–700 °C.
[e] Population of weak acid sites between 100 and 300 °C.
[f] Population of strong acid sites between 300 and 700 °C.

The results of catalytic testing in terms of CO_2 conversion, DME selectivity, methanol selectivity, CO selectivity and DME yield are shown in Table 10. Increasing reaction temperature leads to increasing CO_2 conversion but decreasing DME selectivity. At reaction 260°C, the CZZ-FER catalyst provides the highest DME yield of 14.5% with CO_2 conversion and DME selectivity of 26% and 55.7%., respectively.

Table 10 The results of catalytic testing in terms of CO_2 conversion, DME selectivity, methanol selectivity, CO selectivity and DME yield [16]

Sample	T_R [°C]	X_{CO2} [%]	S_{DME} [%]	S_{MeOH} [%]	S_{CO} [%]	Y_{DME} [%]
CZZ-MOR	200	5.2	78.0	0.7	21.3	4.1
	220	11.2	60.8	4.7	34.5	6.8
	240	17.1	51.0	9.5	39.5	8.8
	260	23.2	50.8	11.2	38.1	11.8
CZZ-FER	200	5.6	79.6	0.2	20.2	4.5
	220	11.7	63.4	3.1	33.5	7.4
	240	20.0	52.4	8.6	39.0	10.5
	260	26.0	55.7	12.8	31.5	14.5
CZZ-MFI	200	4.2	71.0	6.7	22.3	3.0
	220	10.3	51.9	12.1	36.0	5.4
	240	16.9	42.7	11.7	45.6	7.2
	260	21.3	40.5	12.9	46.6	8.6

To illustrated, comparison of the performance and the amount of strong basic and acid sites were considered as shown in Figure 22. The results indicated that increasing amounts of strong basic sites and strong acid sites, led to improve CO_2 conversion and DME formation, respectively.
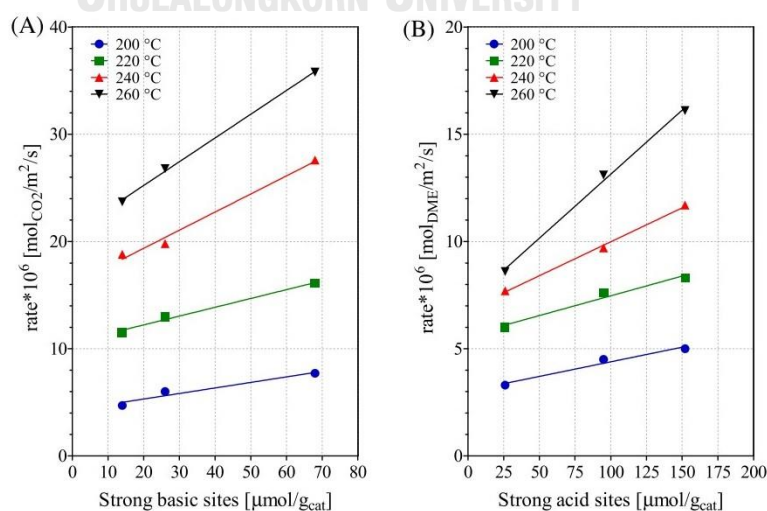
Figure 22 The rate of (A) conversion of CO_2 and (B) formation of DME [16]

After, they investigated the stability of CZZ-FER for a time on stream (TOS) of 150 h. The results are shown in Figure 23, found that the CO_2 conversion, DME selectivity and methanol selectivity dramatic decrease at the first 15 h due to water formed during reaction blocked the active site of catalysts. When complete blockage of active site, the catalyst activity slightly reduced until almost constant.
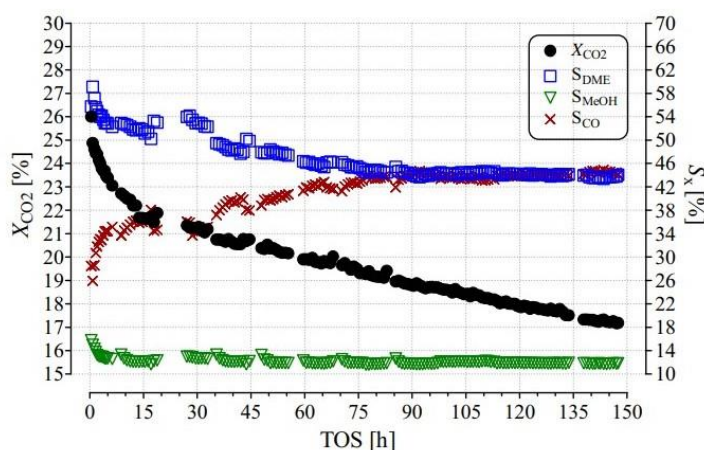
Figure 23 Stability test of CZZ-FER sample [16]

2.4 Alcohol-assisted methanol synthesis

Tsubaki N. et al. [17] proposed a new route of low-temperature methanol synthesis over Cu/ZnO catalyst by using alcohol as a catalytic solvent. A new route reaction composes of 5 steps are shown in Eq. (6)-(10). Comparison of methanol synthesis reaction between the conventional method and low-temperature method are represented in Figure 24.

$$CO + H_2O \longleftrightarrow CO_2 + H_2 \tag{6}$$

$$CO_2 + 1/2H_2 + Cu \longleftrightarrow HCOOCu \tag{7}$$

$$HCOOCu + ROH \longleftrightarrow HCOOR + CuOH \tag{8}$$

$$HCOOR + 2H_2 \longleftrightarrow ROH + CH_3OH \tag{9}$$

$$CuOH + 1/2H_2 \longleftrightarrow H_2O + Cu \tag{10}$$
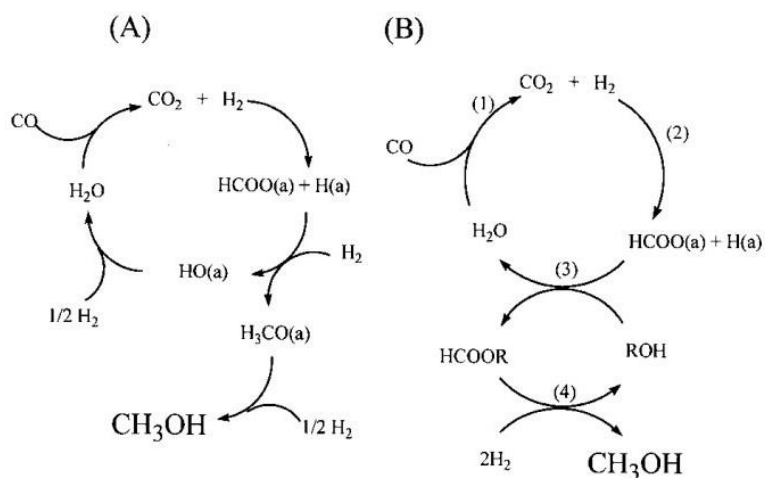
Figure 24 The overall methanol synthesis reaction of (A) conventional method and (B) low-temperature method by addition of alcohol [17]

In the experiment, the Cu/ZnO and Cu/Al$_2$O$_3$ catalysts and ethanol solvent were added into the reactor. The mixture gas of CO/CO$_2$/H$_2$ with 30:5:65 ratio were fed as a reactant gases until the reactor was pressurized to 30 bar then heated the reactor to 150°C. The results are shown in Figure 25, indicated no reaction occur at temperature of 150°C when absence of ethanol. On the contrary, addition of ethanol leads to increasing reactants conversion and methanol yield. This implied that the addition of ethanol made the low-temperature methanol synthesis possible.
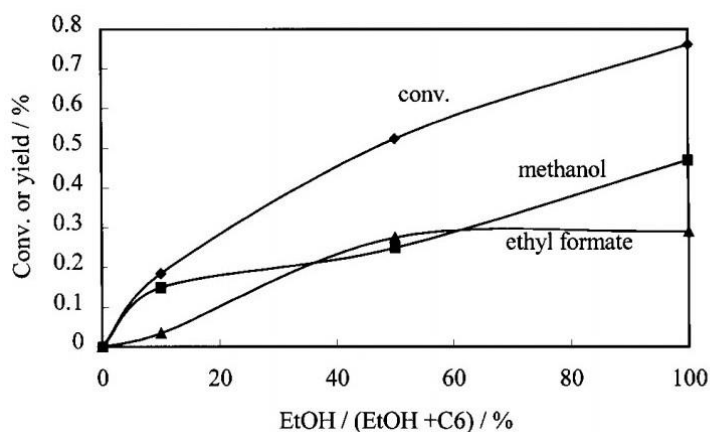
Figure 25 Effect of coexisting alcohol on the conversion and yields [17]

Moreover, Likhittaphon S. et al. [18] studied effect of alcohol type, including ethanol, propanol and butanol for low-temperature alcohol-assisted methanol synthesis at 150°C and 50 bar The results are shown in Figure 26, indicated that ethanol provides the highest methanol yield and methanol selectivity decreases following the larger molecule of alcohol. However, complication in product purification is the main problem of this method when ethanol is used as a catalytic solvent. Ethanol dehydrogenation, unwanted side reaction (Eq. (8)), inevitably occurs under this conditions and ethyl acetate was formed. Methanol and ethyl acetate are azeotrope mixture which is difficult to separate.
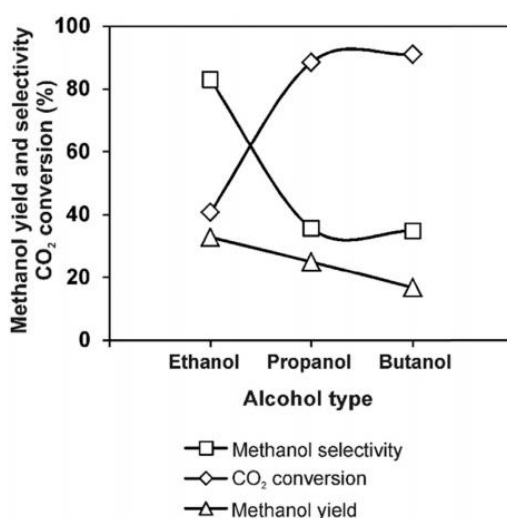
Figure 26 CO_2 conversion and selectivity and yield of methanol various types of alcohol [18]

In this study, methanol was further convert to DME which is gaseous, representing a promising way to mitigate the product purification problem in the new route.

Chapter 3
Research methodology

3.1 Catalyst preparation

3.1.1 CO_2 hydrogenation to methanol catalysts

Cu/ZnO-based catalysts was prepared by co-precipitation method with the mass ratio of Cu/ZnO and Cu/ZnO/ZrO$_2$ was 50:50 and 50:40:10, respectively. Initially, Cu(NO$_3$)$_2$·3H$_2$O (Sigma-Aldrich, 98%), Zn(NO$_3$)$_2$·6H$_2$O (Sigma-Aldrich, 99%) and ZrO(NO$_3$)$_2$·xH$_2$O (Sigma-Aldrich, 99%) were dissolved in deionized (DI) water with concentration of 1 M. The precipitation agent was 1.5 M of Na$_2$CO$_3$ solution. The metal nitrates solution and Na$_2$CO$_3$ solution were dropped into 300 mL of DI water at 65 $^\circ$C and the pH value of the solution was maintained at 8. The precipitate was stirred for 2 h and aged overnight. In the next step, the precipitate was washed with DI water until the conductivity value of the washing water was less than 50 S/m, then centrifuged and dried at 110 $^\circ$C overnight in an oven. Dried sample was ground to powder and calcined at 500 or 700 $^\circ$C with heating rate 10 $^\circ$C/min for 5 h. It is noted that the calcination temperature is obtained from the thermogravimetric analysis. The preparation method of catalysts for CO_2 hydrogenation was summarized in Figure 27.

```
┌─────────────────────────────┐   ┌─────────────────────────┐
│  A mixed solution of Cu and Zn │   │   An aqueous solution   │
│  nitrates + Zr, Al or Zr-Al nitrates │   │     of Na₂CO₃          │
└─────────────────────────────┘   └─────────────────────────┘
```

Figure 27 The summarized of Cu/ZnO-based catalysts preparation

The above flowchart:

Box 1: A mixed solution of Cu and Zn nitrates + Zr, Al or Zr-Al nitrates

Box 2: An aqueous solution of Na$_2$CO$_3$

↓ (both feed into)

Dropped into DI water at 65°C with constant pH value of 8, stirred for 2 h and aged overnight (Co-precipitation method)

↓

Washed, centrifuged and dried at 110°C overnight

↓

Calcined at 500 or 700°C for 5 h

Figure 27 The summarized of Cu/ZnO-based catalysts preparation

3.1.2 Methanol dehydration to DME catalysts

A commercial ZSM-5 (SiO$_2$/Al$_2$O$_3$ molar ratios of 23 and 40) and ferrierite (SiO$_2$/Al$_2$O$_3$ molar ratios of 18) in NH$_4^+$-form purchased from Tosoh Corporation (Japan), were convert to H$^+$-form by calcination at 500°C for 5 h under air.

3.2 Catalyst Characterization

The calcination temperature were determined by Thermogravimetric analysis (TGA, SDT Q600). Scanning electron microscopy with energy dispersive X-ray (SEM-EDX) were used to investigate morphology (Hitachi, S3400) and atomic composition on catalysts surface (EDAX, Apollo x). Surface area, pore size and pore volume were determined by N$_2$ adsorption with Brunauer-Emmett-Teller (BET) method (Micromeritics, ASAP 2020).

Crystallinity of catalysts were analyzed by X-ray diffraction (XRD, Bruker AXS, D8 Advance) in the 2θ range 20-80°. Then crystallites size were calculated from Scherrer's equation (Eq. (11))

$$L = \frac{K\lambda}{\beta_{FWHM}\cos\theta} \tag{11}$$

where L is the crystallites size in nanometer, K is a shape factor (K=0.9 for spherical particles), λ is wavelength of radiation (λ=1.54178 Å), β_{FWHM} is Full width half maximum in radians, θ is the peak position in degree.

The reduction temperature were determined by temperature program of reduction (H_2-TPR) using Micromeritics, Chemisorb 2750 with gas flow rate 25 mL/min and heating rate of 10°C/min. Catalysts of 0.05 g were loaded into a glass U-tube reactor and dried at 300°C for 1 h in N_2 flow. After cooled down, reactor was heated to 550°C with 10%H_2/Ar flow.

The acidity was analyzed by NH_3 temperature program of desorption (NH_3-TPD) using Micromeritics, Chemisorb 2750 with gas flow rate 25 mL/min and heating rate of 10°C/min. Catalysts of 0.04 g were loaded into a quartz U-tube reactor and dried at 300°C for 1 h in He flow. After cooled down to room temperature, NH_3 were fed to be adsorbed on the acid sites of catalysts for 1 h. Then reactor was heated to 850°C with He flow to desorbed NH_3. The amount of acid sites were calculated by curve deconvolution.

3.3 Catalyst testing

3.3.1. Methanol dehydration to DME

To select a suitable zeolites including ZSM-5 (SAR=23), ZSM-5 (SAR=40) or ferrierite (SAR=18), the methanol dehydration reaction was initially tested. The bare zeolites were tested toward the methanol dehydration to DME. 80 mL of methanol and 3 g of zeolite were added to the autoclave reactor. Nitrogen gas (N_2) gas was fed to the reactor with the flow rate of 100 mL/min until the reactor was pressurized to 15 bar. When the operating temperature increased to 150°C, the pressure increased to 35 bar. The reaction was carried out at 150°C with vigorous stirring 500 rpm for 4 h. Finally, the effluent products were analyzed by an on-line gas chromatography (SHIMADSU Nexis GC-2030) with mid-polar SH-Rtx^{TM}-624 column. The methanol conversion and DME yield were calculated.

3.3.2 DME synthesis from CO_2 through an ethanol-assisted method

DME synthesis from CO_2 was divided into two steps: ethanol-assisted methanol synthesis and DME synthesis. Firstly, Cu/ZnO-based catalyst was reduced by H_2/N_2 in fixed bed reactor at 250 - 350°C for 3 h under atmospheric pressure. CO_2 hydrogenation to methanol reaction through an ethanol-assisted method was investigated in an autoclave batch reactor. 3 g of catalyst and 100 mL of ethanol were loaded in the reactor, then CO_2/H_2 with molar ratio 1:3 were fed as the reactant gases until the reactor was pressurized to about 36 bar. After that, heated the reactor to 150°C. When the temperature reached 150 °C, the reactor pressure was increased to 50 bar. The reaction was carried out for 24 h with vigorous stirring 500 rpm before cooled down to room temperature. The effluent products were sampled and analyzed by gas-chromatography. Then CO_2 conversion and methanol yield were calculated.

Finally, 80 mL of residue effluent products were filtered to remove solid catalyst and loaded in the reactor as the reactant for methanol dehydration to DME. The method was same as mentioned in section 3.2.1. The schematic drawing and summarized of the system for DME synthesis from CO_2 are presented in Figure 28 and 29, respectively.
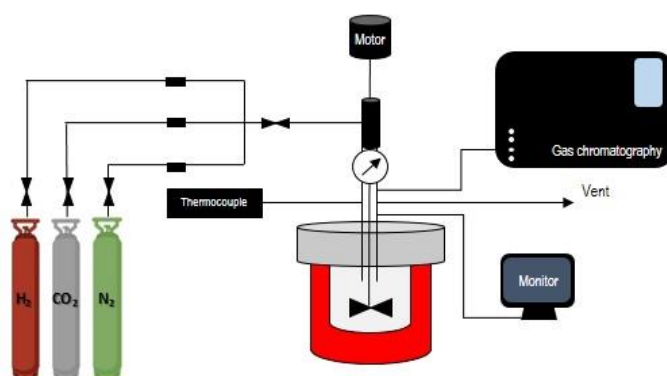
Figure 28 The schematic drawing of the system

Reduce Cu/ZnO- based catalyst by H_2/N_2 in fixed-bed reactor at 250 - 300°C for 3 h

Loaded catalyst and ethanol into the reactor

Fed CO_2/H_2 with molar ratio 1:3 until the reactor was pressurized to 35 bar and heated to 150°C

The reaction was carried out for 24 h with vigorous stirring 500 rpm then cooled down

80 mL of residue effluent products were filtered to remove catalyst and loaded in the reactor with 3 g of zeolite

Analyzed some of effluent products with gas-chromatograph and calculated CO_2 conversion and methanol yield

Fed N_2 until the reactor was pressurized to 15 bar and heated to 150°C

The reaction was carried out for 4 h with vigorous stirring 500 rpm then cooled down

Effluent products were analyzed with gas-chromatography then calculated DME yield

Figure 29 The summarized of CO_2 hydrogenation to methanol through an ethanol-assisted method

Chapter 4

Results and Discussion

4.1 Methanol dehydration to DME

4.1.1 Effect of zeolite types

The various types of zeolites including ZSM-5 (SAR=23 and 40) and ferrierite (SAR=18) were characterized by SEM, BET and NH_3-TPD techniques.

SEM images are shown in Figure 30. It was clearly seen that various zeolite presented different morphology. ZSM-5 (SAR=23) consists of rod-like crystallites agglomerated with small spherical particles as shown in Figure 30(a)-(b), while ZSM-5 (SAR=40) consists of cubic-like crystallites as shown in Figure 30(c)-(d). Ferrierite (SAR=18) consisted mainly of thin-plate shaped as shown in Figure 30(e)-(f). This results indicated that different SiO_2/Al_2O_3 ratio (SAR) affected the structural morphology, and led to the different surface area as shown in Table 11. The ZSM-5 (SAR=23) exhibited the highest BET surface area followed by the ZSM-5 (SAR=40) and the ferrierite (SAR=18) of 343.1, 313.6 and 261.9 m^2/g, respectively.
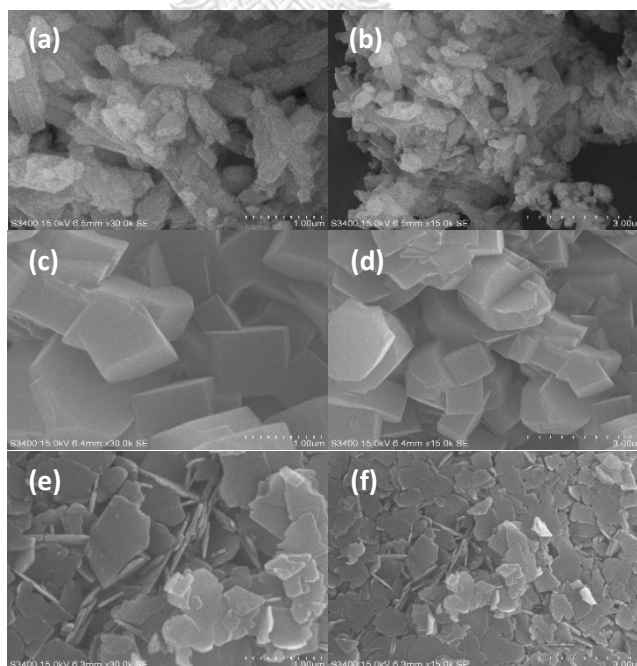
Figure 30 SEM images of (a-b) ZSM-5 (SAR=23), (c-d) ZSM-5 (SAR=40) and (e-f) ferrierite (SAR=18)

Table 11 BET surface area and the amount of acid sites of various zeolites

Samples	SiO_2/Al_2O_3 ratio	S_{BET} (m^2/g)	Total acid capacity	Weak sites	Strong sites
			(mmol/g_{cat})		
ZSM-5	23	343.1	20.636	12.562	8.074
ZSM-5	40	313.6	19.016	11.902	7.114
Ferrierite	18	261.9	23.738	13.874	9.864

The NH_3-TPD profiles of various zeolites, shown in Figure 31, composed mainly 2 desorption peaks of weak acid sites (50-350°C) and strong acid sites (350-600°C). The peaks of ferrierite presented stronger acid strength and displayed slightly shift to the higher temperature when compared with other zeolites. The corresponding the amount of acid was calculated by curve deconvolution as shown in Table 11. The ferrierite (SAR=18) had the highest total acid capacity of 23.738 mmol/g_{cat} followed by ZSM-5 (SAR=23) and ZSM-5 (SAR=40), respectively. This implied that the SiO_2/Al_2O_3 ratio affected the acid strength of zeolites, it was likely that increasing the aluminium content led to a stronger acid strength [19].

In addition, the lower temperature was known to associate with the Lewis acid sites while the higher temperature is ascribed to the Brønsted acid sites [20]. The active sites that metal cations such as Si^+ and Al^+ accept electrons were the Lewis acid sites while the Brønsted acid sites contain hydroxyl groups on the surface and can donate protons [21]. The Brønsted acid sites are more active for alcohol dehydration reaction [22]. Protons (H^+) on the Brønsted acid sites are donated to the hydroxyl group (OH^-) of methanol (CH_3OH) to produce water (H_2O). Then the residue alkyl group (-CH_3) on the catalyst surface react with another molecule of methanol to produce DME (CH_3OCH_3).
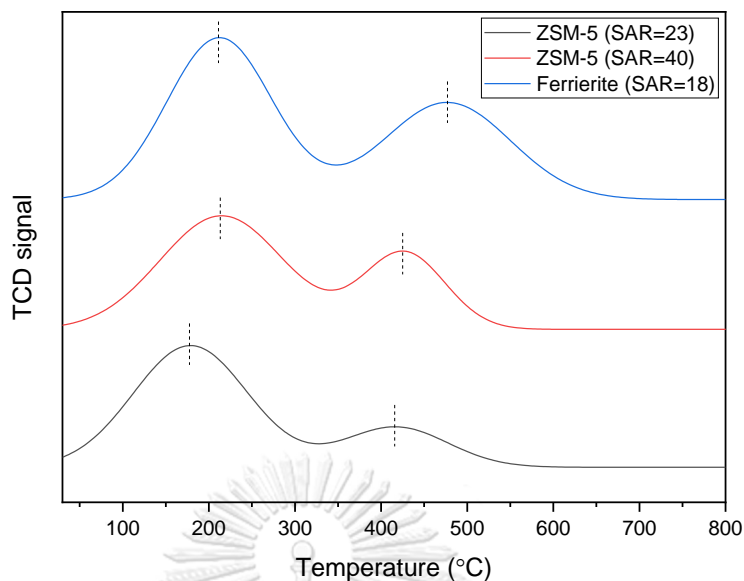
Figure 31 NH$_3$-TPD profiles of ZSM-5 (SAR=23), ZSM-5 (SAR=40) and ferrierite (SAR=18)

Figure 32 presents the results of catalytic testing for methanol dehydration to DME reaction at 150°C and pressure of 35 bar. The results indicated that ferrierite provided the highest methanol conversion and DME yield of 47.09 and 2.69%, respectively, followed by ZSM-5 (SAR=40) and ZSM-5 (SAR=23). According to the work of Frusteri et al. [16], ferrierite was reported to provide high DME yield of 14.5%, while ZSM-5 provides 8.6% DME yield at reaction temperature of 260°C. The DME yield was reported to decrease with reaction temperature. At 200°C, DME yield decreases to 4.5 and 3% for ferrierite and ZSM-5 system, respectively [16]. In this study, pressurized reactor was used and due to its limitation, the reaction temperature was not increased more than 150°C. Although ferrierite has the lowest surface area, it provided the highest methanol conversion and DME yield since it had the strongest acid sites. This implied that the acid strength had more influence on the catalytic performance, corresponding to the work of Ramos et al. [15] which presents the stronger acid sites provided more activity of catalysts.
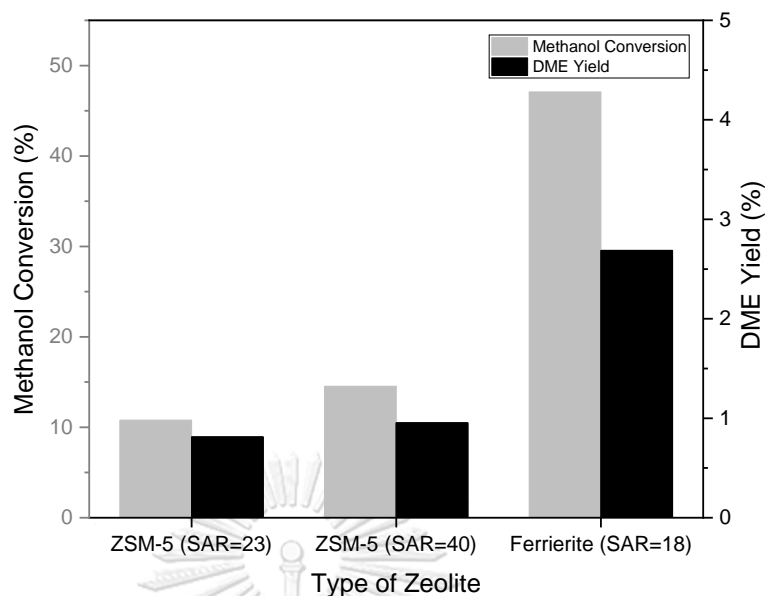
Figure 32 Methanol conversion and DME yield of various type of zeolites for methanol dehydration reaction

4.1.2 Effect of reaction pressure

Generally, methanol dehydration to DME reaction is carried out in gas phases using a fixed-bed reactor at atmospheric pressure since operating pressure has been reported no effect on this reaction [19, 23]. Moreover, according to (Eq. (2)) the moles of reactant is equal to moles of product, according to Le Chatelier's principle, indicating no effect of pressure. However, in this study, the reaction was carried out in an autoclave which contained ethanol as a catalytic solvent. The reactor was designed for low-temperature methanol synthesis which was carried out in a batch reactor. Ferrierite catalyst was added in the reactor. As shown in Figure 33, no reaction occurred without pressurization because at reaction temperature of 150℃ methanol in gas phase could not reach the catalyst which was located at bottom of the reactor. Pressurizing higher than saturated vapor pressure, as calculated by Antoine's equation, in order to prevent phase change of methanol [22].

The reactor was initially pressurized by N_2 to 10, 15 and 20 bar and then temperature was increased. When temperature reached 150 ℃, the reactor pressure was 30, 35 and 40 bar, respectively. Methanol is liquid phase in this pressurizing

conditions. As shown in Figure 34, methanol conversion and DME yield insignificantly change with pressure. Methanol conversion was 47.61, 47.09 and 43.93%, while DME yield was 2.22, 2.69 and 2.22% for pressure of 30, 35 and 40 bar, respectively. This indicated that the pressure has no significant effect on this reaction, if the reactor was pressurized higher than the saturated vapor pressure of methanol (14.04 bar, calculated from Antoine's equation).
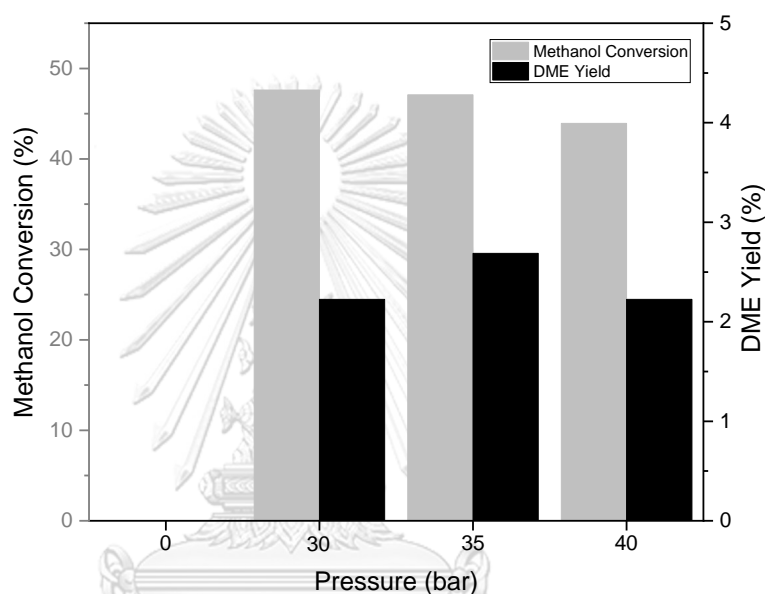
Figure 33 Methanol conversion and DME yield of various operating pressure for methanol dehydration reaction

4.1.3 Effect of reaction Temperature

Effect of reaction temperature on methanol dehydration was investigated in a range 110-150℃. The ferrierite catalyst was used and the reactor was initially pressurized to 15 bar. When the reactor was heated to a desired temperature of 110, 130 and 150℃, the reactor pressure was 21, 24 and 35 bar, respectively. As shown in Figure 34, increasing reaction temperature led to a higher methanol conversion and DME yield. The methanol conversion at the reaction temperature of 110, 130 and 150℃ were 10.18, 13.34 and 47.09% and the DME yield were 0.42, 1.30 and 2.69%, respectively. According to the work of Catizzone et al. [19], methanol conversion in dehydration reaction in the temperature range 120-240℃ increases with increasing

operating temperature. However, light hydrocarbon is formed as by-product, i.e. methane and ethylene, when the operating temperature was higher than 240°C. Moreover, the work of Hammond et al. [24] reported few of methane and ethylene production at reaction temperature below 400°C and dramatic increase at 450°C. Therefore, lower reaction temperature is suitable for DME production [19, 25]. Methanol dehydration to DME reaction (Eq. (2)) is exothermic reaction (ΔH°_{298} = -23.4 kJ/mol). The equilibrium conversion is limited at high temperature.

In this study, DME synthesis at reaction temperature 150°C provided the highest methanol conversion and DME yield without by-product formation.
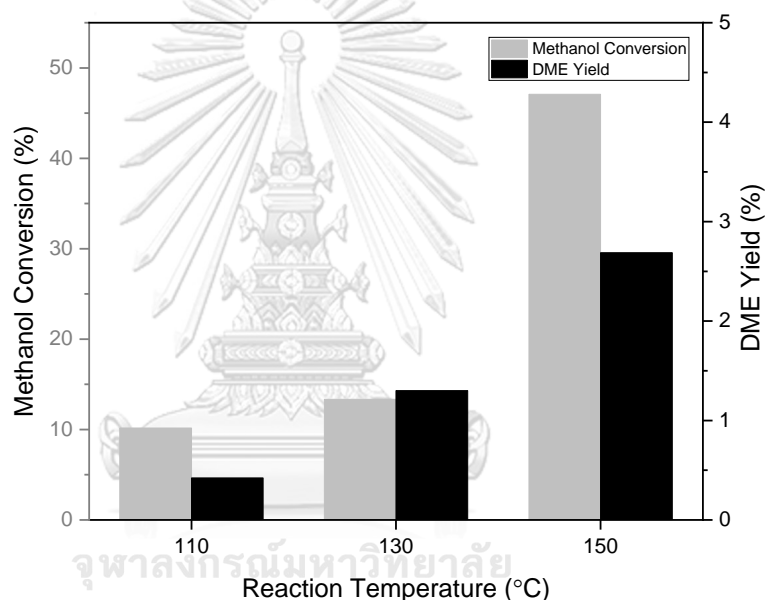
Figure 34 Methanol conversion and DME yield of various reaction temperature for methanol dehydration reaction

4.2 DME synthesis from two-step method: ethanol-assisted methanol synthesis and methanol dehydration

DME was synthesized from CO_2 and H_2 through two-step method. In the first step, methanol was synthesized through ethanol-assisted method using Cu/ZnO-based catalysts. In the second step, methanol dehydration was carried out using ferrierite catalyst.

4.2.1 Characterization of Cu/ZnO-based catalysts

The Cu/ZnO, Cu/ZnO/ZrO$_2$, Cu/ZnO/Al$_2$O$_3$ and Cu/ZnO/ZrO$_2$/Al$_2$O$_2$ catalysts were characterized by TGA, SEM-EDX, XRD, BET and H$_2$-TPR techniques. The TGA patterns of Cu/ZnO-based catalysts are shown in Figure 35. The results show that Cu/ZnO and Cu/ZnO/ZrO$_2$ catalysts can be calcined at 500℃ while Cu/ZnO/Al$_2$O$_3$ and Cu/ZnO/ZrO$_2$/Al$_2$O$_3$ catalysts can be calcined at 700℃ in ambient air to complete decomposition of impurities.
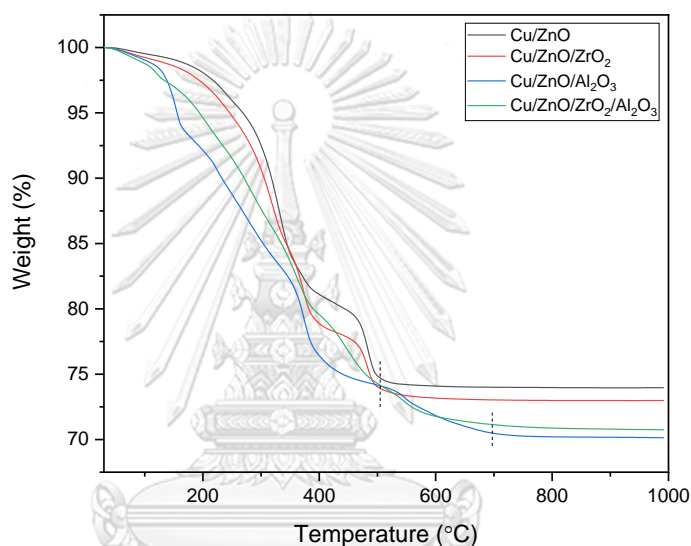
Figure 35 TGA patterns of Cu/ZnO-based catalysts

SEM images and EDX mapping of calcined Cu/ZnO, Cu/ZnO/ZrO$_2$, Cu/ZnO/Al$_2$O$_3$ and Cu/ZnO/ZrO$_2$/Al$_2$O$_3$ catalysts are shown in Figure 36-39, respectively. The EDX mapping presented well-dispersion of all catalysts while the SEM images display different morphology of various catalysts. Cu/ZnO catalyst in Figure 36 (a)-(b) consisted of mainly agglomerated spherical particles. Cu/ZnO/ZrO$_2$ catalyst in Figure 37 (a)-(b) illustrated a flake-like morphology. Cu/ZnO/Al$_2$O$_3$ catalyst in Figure 38 (a)-(b) presented rod-shaped crystallites. Cu/ZnO/ZrO$_2$/Al$_2$O$_3$ catalyst in Figure 39 (a)-(b) exhibited rod-shaped crystallites agglomerated with small spherical particles. This indicated that addition of various promoters affected catalyst morphology, leading to different surface area as shown in Table 12. The addition of ZrO$_2$ led to more flake-like morphology while Al$_2$O$_3$ led to more rod-like crystallites of catalysts. Moreover,

EDX technique presented the composition of elements in the catalyst as shown in Table 12. The element composition was rather proportional as it was intended to be synthesized.

Surface area of catalysts analyzed by BET technique are shown in Table 12, reveals $Cu/ZnO/ZrO_2$ catalyst has the highest surface area, pore volume and pore size of 35.42 m^2/g, 0.28 cm^2/g and 314.81 Å, followed by $Cu/ZnO/ZrO_2/Al_2O_3$, Cu/ZnO and $Cu/ZnO/Al_2O_3$. The surface area of $Cu/ZnO/ZrO_2/Al_2O_3$, Cu/ZnO and $Cu/ZnO/Al_2O_3$ were 34.35, 21.81 and 18.7 m^2/g, respectively.
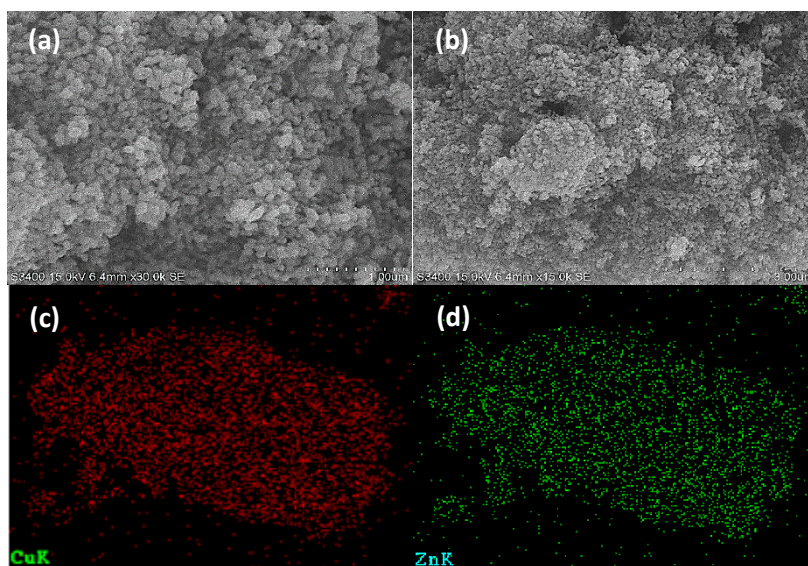
Figure 36 SEM images of (a-b) calcined Cu/ZnO catalyst; EDX mapping of (c) Cu and (d) ZnO
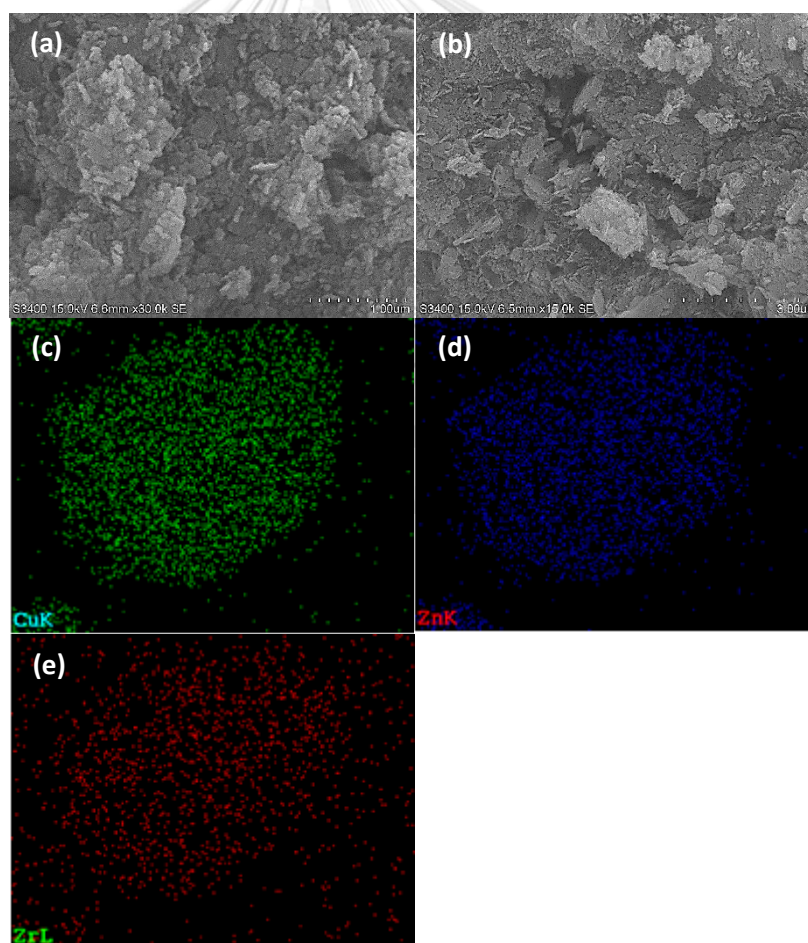
Figure 37 SEM images of (a-b) calcined Cu/ZnO/ZrO$_2$ catalyst; EDX mapping of (c) Cu, (d) ZnO and (e) ZrO$_2$
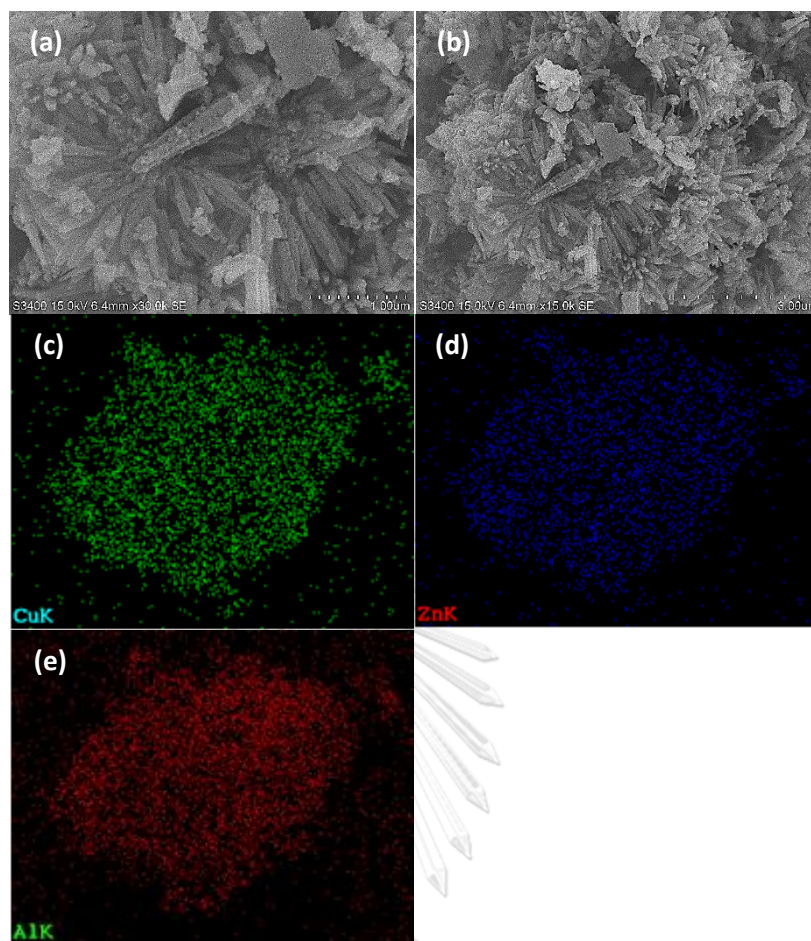
Figure 38 SEM images of (a-b) calcined Cu/ZnO/Al$_2$O$_3$ catalyst; EDX mapping of (c) Cu, (d) ZnO and (e) Al$_2$O$_3$
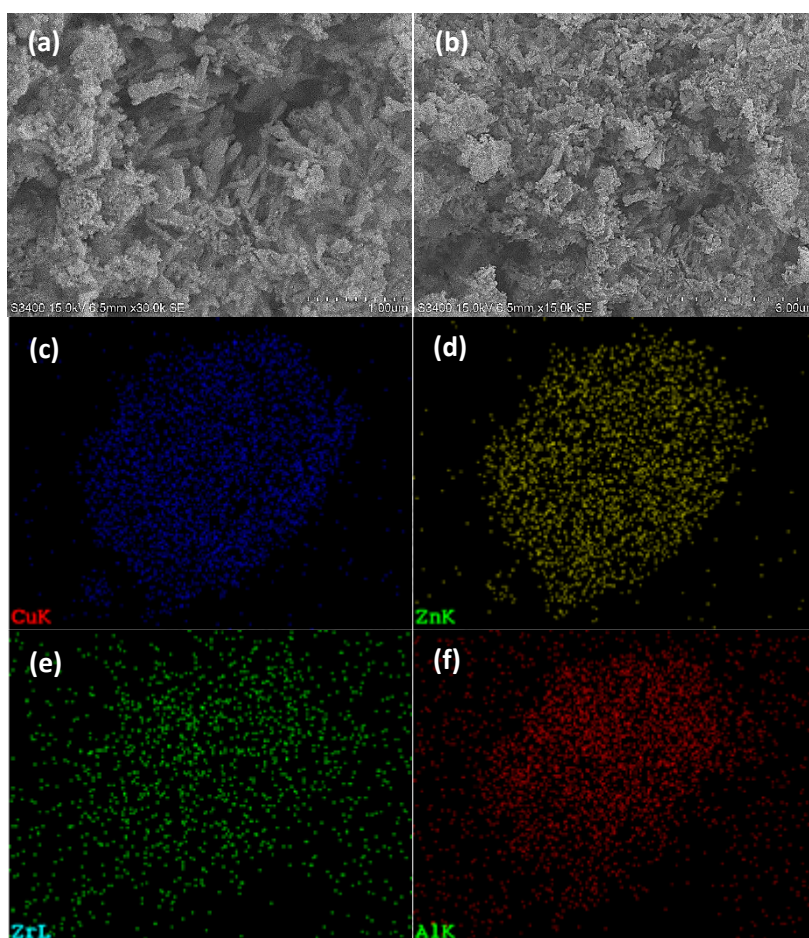
Figure 39 SEM images of (a-b) calcined Cu/ZnO/ZrO$_2$/Al$_2$O$_3$ catalyst; EDX mapping of (c) Cu, (d) ZnO, (e) ZrO$_2$ and (f) Al$_2$O$_3$

Table 12 Properties of Cu/ZnO-based catalysts

Sample	Composition				S$_{BET}$	Pore Volume	Pore Size	CuO Crystallite size	ZnO Crystallite Size
	Cu	ZnO	ZrO$_2$	Al$_2$O$_3$	(m^2/g)	(cm^2/g)	(Å)	(nm)	(nm)
Cu/ZnO	50.35	45.65	-	-	21.811	0.047	86.654	14.301	17.742
Cu/ZnO/ZrO$_2$	48.99	40.97	10.04	-	35.417	0.279	314.806	8.637	7.809
Cu/ZnO/Al$_2$O$_3$	50.06	39.08	-	10.86	18.699	0.065	139.555	20.272	14.678
Cu/ZnO/ZrO$_2$/Al$_2$O$_3$	50.56	40.58	4.05	4.81	34.353	0.132	153.239	18.556	27.513

The XRD patterns of calcined Cu/ZnO-based catalysts are shown in Figure 40. The peak position at 2θ was 35.6, 38.8, 48.6, 53.6, 58.3, 61.5 and 66.2°, represent the crystallites of CuO while ZnO crystallites display at the peak position of 2θ are 31.8,

34.4, 36.2, 47.5, 56.6, 62.9 and 68.0° [11]. The peaks of ZrO_2 and Al_2O_3 were not observed, implying highly dispersion in amorphous form of ZrO_2 and Al_2O_3 in the catalysts [26].

Cu/ZnO/ZrO_2 catalyst exhibited broader peaks of CuO and ZnO, indicated that the addition of ZrO_2 led to a smaller crystallites size. According to Table 12, the CuO and ZnO crystallites size of Cu/ZnO/ZrO_2, which calculated from Scherrer equation, were smaller than Cu/ZnO of 5.66 and 9.93 nm, respectively. Thus the surface area of Cu/ZnO/ZrO_2 was also relatively high.

The addition of Al_2O_3 led to the sharper peaks of CuO but the broader peaks of ZnO, indicating a bigger CuO crystallites size and a smaller ZnO crystallites size. However, the surface area of Cu/ZnO/Al_2O_3 was lower than that of Cu/ZnO, implying that CuO crystallites size had more impact than the ZnO crystalltes size on the surface area as shown in Table 12.
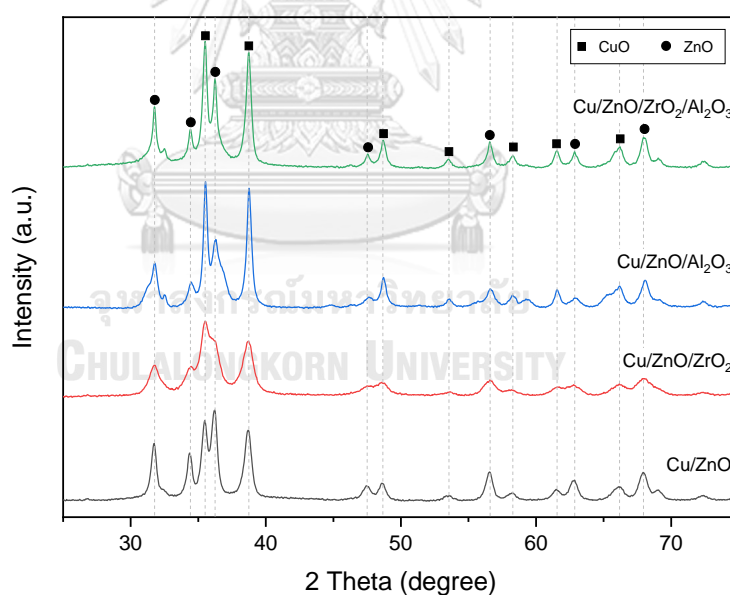
Figure 40 XRD patterns of the calcined Cu/ZnO-based catalysts

The H_2-TPR profiles are shown in Figure 41, displaying the main peak of CuO reduction to Cu at the temperature range of 150-360°C [27]. From this result, Cu/ZnO/ZrO_2, Cu/ZnO, Cu/ZnO/ZrO_2/Al_2O_3 and Cu/ZnO/Al_2O_3 catalysts were completely reduced to Cu form at temperature of 250, 280, 340 and 360°C,

respectively. $Cu/ZnO/ZrO_2$ catalyst exhibited a shift to the lowest temperature. This indicated that addition of ZrO_2 led to the easier reduction of CuO since it helped decreasing CuO crystallites size [11] while Al_2O_3 addition led to harder reduction since the CuO crystallites size was increased.
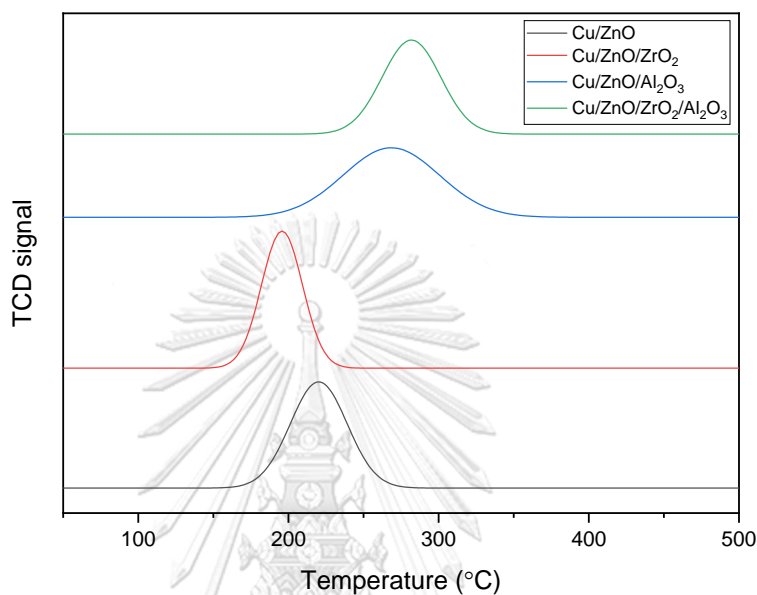
Figure 41 H_2-TPR profiles of Cu/ZnO-based catalysts

3.2.2 Ethanol-assisted methanol synthesis and methanol dehydration

The results of CO_2 hydrogenation to methanol through an ethanol-assisted method over Cu/ZnO-based catalyst at temperature of 150°C and pressure of 50 bar for 24 hours on the first stage are shown in Figure 42. The result shows that $Cu/ZnO/ZrO_2$ catalyst provided the highest activity for the ethanol-assisted methanol synthesis followed by $Cu/ZnO/ZrO_2/Al_2O_3$, Cu/ZnO and $Cu/ZnO/Al_2O_3$. The CO_2 conversion were 82.1, 81.8, 76.7 and 71.6%, while yield of methanol were 60.8, 49.8, 49.4 and 37.9% for $Cu/ZnO/ZrO_2$, $Cu/ZnO/ZrO_2/Al_2O_3$, Cu/ZnO and $Cu/ZnO/Al_2O_3$ catalyst, respectively. This result related to catalytic characterization as mentioned earlier, $Cu/ZnO/ZrO_2$ catalyst had the highest surface area and the smallest CuO crystallites size led to the highest CO_2 conversion and methanol yield. Comparing to a conventional methanol synthesis through CO_2 hydrogenation as shown in Table 13, it is clear that the ethanol-assisted methanol synthesis leads to possible a lower-

temperature pathway and more yield of methanol. For example, Fang et al. [28] reports the results of CO_2 hydrogenation which was carried out in fixed-bed reactor at 250°C and 50 bar. The results shows that $Cu/ZnO/ZrO_2$ catalyst provided methanol yield merely of 5.2%.
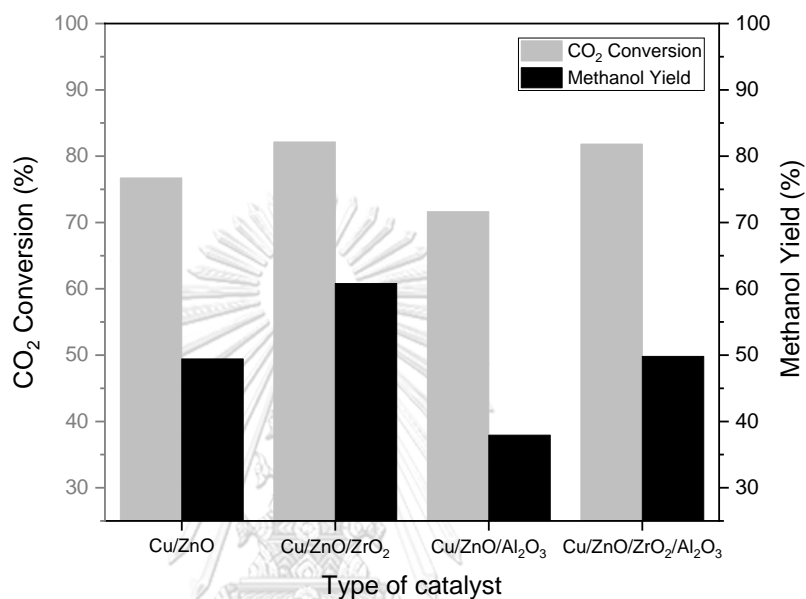
Figure 42 CO_2 conversion and methanol yield of various Cu/ZnO-based catalysts for CO_2 hydrogenation to methanol through an ethanol-assisted method in the first stage

Table 13 Comparisons of methanol yield in conventional methanol synthesis

Catalyst	Operating condition		% Yield of methanol	Reference
	Temperature (°C)	Pressure (bar)		
Cu/ZnO	240	45	9.0	[29]
Cu/ZnO	280	30	4.3	[30]
$Cu/ZnO/ZrO_2$	250	50	5.2	[28]
$Cu/ZnO/ZrO_2$	250	30	7.9	[31]
$Cu/ZnO/Al_2O_3$	220	28	12.8	[32]
$Cu/ZnO/Al_2O_3$	250	30	4.3	[33]
$Cu/ZnO/ZrO_2/Al_2O_3$	220	28	12.4	[12]
$Cu/ZnO/ZrO_2/Al_2O_3$	250	50	17.9	[34]

In the second stage, effuent products were used as reactants for methanol dehydration to DME over ferrierite catalyst in the operating conditions at 150°C and 35 bar for all systems. The DME productivity are shown in Figure 43. The results indicate that $Cu/ZnO/ZrO_2$ with ferrierite system provided the highest DME productivity of 0.4385 $mmol_{DME}/g_{cat}$, followed by $Cu/ZnO/ZrO_2/Al_2O_3$, Cu/ZnO and $Cu/ZnO/Al_2O_3$, respectively. This results related to the CO_2 conversion and the methanol yield in the first stage where the $Cu/ZnO/ZrO_2$ catalyst provided the highest amount of methanol leading to the highest DME production. However, when considering the DME yield toward methanol reactant, the DME yield of the $Cu/ZnO/ZrO_2$ system was slightly lower than the others since there was the highest amount of methanol reactant in this system.

Furthermore, under this experiment, ethylene was detected. It was likely to be generated as a valued by-product through ethanol dehydration to ethylene reaction over zeolite catalyst [35]. The productivity and yield of ethylene are about 5.45 $mmol_{Ethylene}/g_{cat}$ or 1.33% yield based on ethanol reactant for all systems as shown in Figure 43 and 44, respectively. Although the amount of ethylene were higher than

DME, it has lower yield. This because there was a larger amount of ethanol than methanol in the system. To gain more yield of ethylene, the ethanol dehydration reaction could be enhanced by increasing reaction temperature. According to the work of Golabek et al. [36], temperature of 240-260°C could enhanced methanol dehydration to DME reaction. Catizzone [37] and Aloise [38] et al. also presented methanol conversion was the highest at reaction temperature of 240°C. However, the product separation of system which contained DME, ethylene, methanol and ethanol were not complicate since the boiling point of each substance are quietly different. The boiling point of ethylene, DME, methanol and ethanol are -103.7, -24, 64.7 and 78.3°C, respectively. Therefore, the calculation of energy consumption and economic analysis should be studied for feasible consideration in the future.

In addition, for methanol synthesis in the first stage, the Henry's constant value of CO_2 and H_2 are different. The Henry's constant value of CO_2 and H_2 are 0.035 and 0.00078 mol kg^{-1} bar^{-1}, respectively. This led to CO_2 have higher solubility than H_2 under the same temperature and pressure. Therefore, the effect of the molar ratio of CO_2 and H_2 which dissolved in catalytic solvent as ethanol should be further studied.
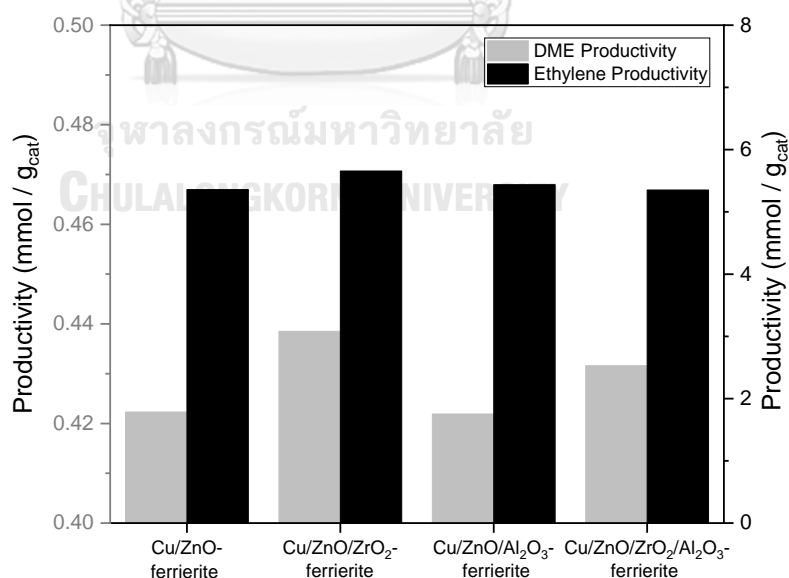
Figure 43 Productivity of DME and ethylene of various Cu/ZnO-based system for methanol dehydration to DME over ferrierite catalyst in the second stage
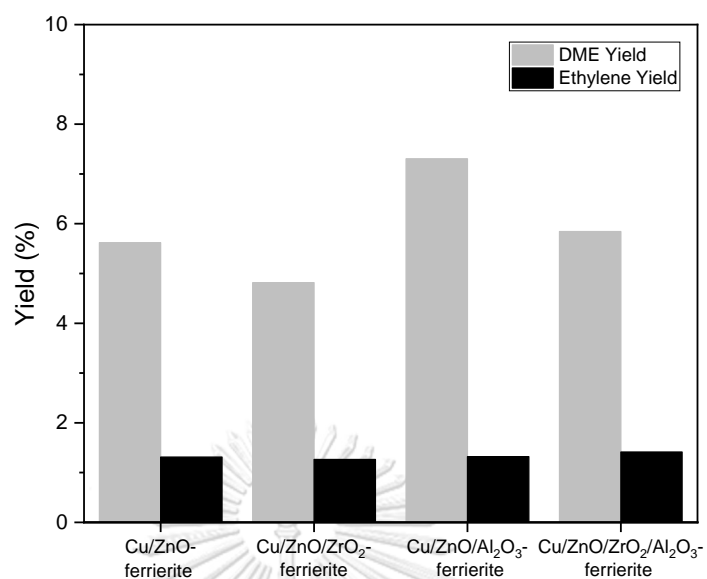
Figure 44 Yield of DME and ethylene of various Cu/ZnO-based system for methanol dehydration to DME over ferrierite catalyst in the second stage

Chapter 5

Conclusion

Ferrierite provided better catalytic activity for methanol dehydration when compared with ZSM-5. ZSM-5 Various SiO_2/Al_2O_3 displayed clearly different structural morphology and led to different surface area and activity of catalyst. Although, ferrierite had the lowest surface area but it had the highest amount of acid sites. This implied that the acid strength has a significant impact on catalytic activity than surface area in DME synthesis. At 150°C was optimal operating temperature, while pressure had no significant impact on this reaction.

Cu/ZnO-based catalysts and ferrierite were investigated for two steps DME synthesis from CO_2. The results indicated that $Cu/ZnO/ZrO_2$ catalyst presented higher CO_2 conversion and methanol yield of 82.1% and 60.8%, followed by $Cu/ZnO/ZrO_2/Al_2O_3$, Cu/ZnO and $Cu/ZnO/Al_2O_3$, respectively. This related to catalytic characterization, addition of ZrO_2 could improve catalytic activity for methanol synthesis due to decreased CuO crystallites size and increased surface area of catalyst while Al_2O_3 addition provided contrary effect. Therefore, $Cu/ZnO/ZrO_2$ system provided the highest DME productivity for methanol dehydration reaction in the second stage.

Moreover, there are ethanol dehydration reaction occurred as a side-reaction to produced ethylene as a valued by-product of 1.33% yield for all system in the second stage.

REFERENCES

Appendix A

Other Results

A.1 Standard Calibration curve of substance
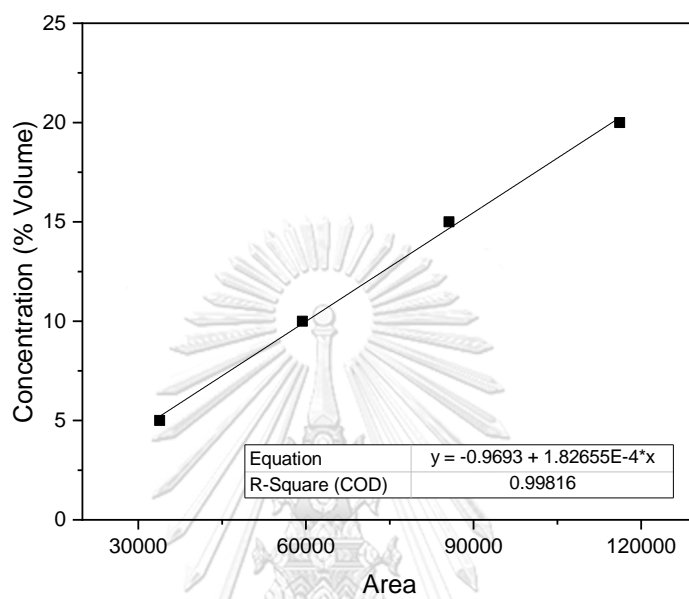
Figure 45 Standard calibration curve of CO_2
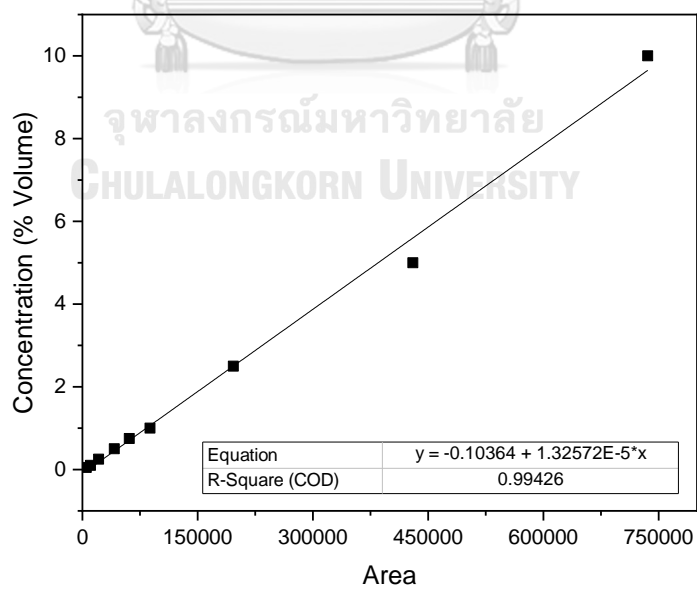
Figure 46 Standard calibration curve of methanol
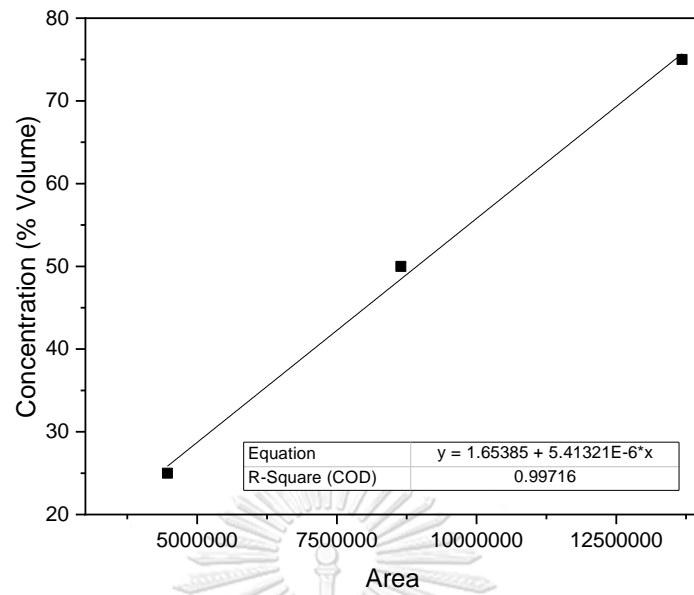
Figure 47 Standard calibration curve of ethanol
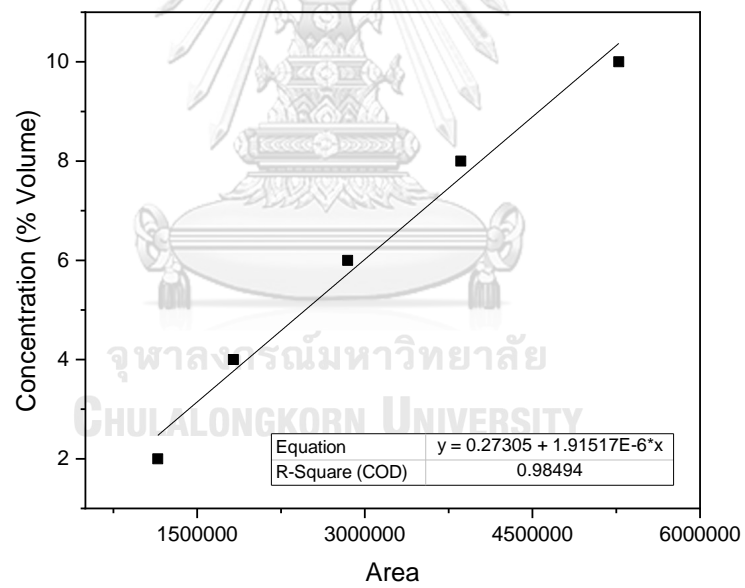
Figure 48 Standard calibration curve of DME
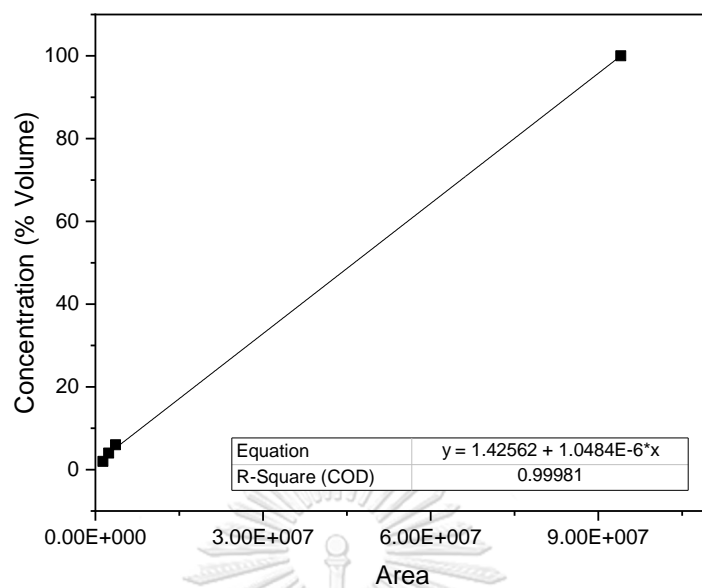
Figure 49 Standard calibration curve of ethylene

A.2 Summary results of testing

Table 14 Results of methanol dehydration to DME

Variation	Catalyst	Operating conditions			%Conversion of methanol	%Yield of DME	Productivity of DME (mmol$_{DME}$/g$_{cat}$)
		Temperature (°C)	Pressure (bar)	Time (h)			
Type of zeolite	ZSM-5 (SAR=23)	150	35	4	10.78899	0.81305	5.32084
	ZSM-5 (SAR=40)	150	35	4	14.53285	0.9537	6.24147
	Ferrierite (SAR=18)	150	35	4	47.08645	2.6866	17.58212
Reaction pressure	Ferrierite (SAR=18)	150	30	4	47.61472	2.2245	14.55808
	Ferrierite (SAR=18)	150	35	4	47.08645	2.6866	17.58212
	Ferrierite (SAR=18)	150	40	4	43.92848	2.22453	15.37099
Reaction temperature	Ferrierite (SAR=18)	110	21	4	10.17514	0.42198	2.76158
	Ferrierite (SAR=18)	130	24	4	13.34387	1.301	8.51126
	Ferrierite (SAR=18)	150	35	4	47.08645	2.6866	17.58212

Table 15 Results of two-step method for DME synthesis from CO_2

Ethanol-assisted methanol synthesis (1st stage)			Methanol dehydration to DME (2nd stage)				
Catalyst	%Conversion of CO_2	%Yield of methanol	Catalyst	%Yield of DME	%Yield of ethylene	Productivity of DME ($mmol_{DME}/g_{cat}$)	Productivity of ethylene ($mmol_{ethylene}/g_{cat}$)
Cu/ZnO	76.70741	49.4368	Ferrierite (SAR=18)	5.6195	1.313	0.4223	5.3571
Cu/ZnO/ZrO$_2$	82.1367	60.8011	Ferrierite (SAR=18)	4.8161	1.2643	0.4385	5.656
Cu/ZnO/Al$_2$O$_3$	71.62325	37.94195	Ferrierite (SAR=18)	7.3037	1.3214	0.4219	5.438
Cu/ZnO/ZrO$_2$/Al$_2$O$_3$	81.82573	49.8174	Ferrierite (SAR=18)	5.8434	1.4151	0.4316	5.351

Appendix B

Calculation

B.1 Saturated vapor pressure calculation by Antoine's Equation

$$\log P = A - \frac{B}{C + T} \qquad \text{(B-1)}$$

P is the saturated vapor pressure in kPa

T is temperature in Kelvin

A, B and C are the Antoine's coefficient (For methanol: A=7.20519, B=1581.993 and C=-33.289)

At 150°C, the saturated vapor pressure of methanol is 14.04 bar

B.2 Crystallite size calculation by Scherrer's Equation

$$L = \frac{K\lambda}{\beta_{FWHM} \cos\theta} \qquad \text{(B-2)}$$

L is the crystallites size in nanometer

K is a shape factor (K=0.9 for spherical particles)

λ is wavelength of radiation (λ=1.54178 Å)

β_{FWHM} is Full width half maximum in radians

θ is the peak position in degree

B.3 The percent of conversion, yield and productivity calculation

$$\% \ CO_2 \ \text{Conversion} = \frac{\text{mole of reacted } CO_2}{\text{mole of initial } CO_2} \times 100 \qquad \text{(B-3)}$$

$$\% \text{ Methanol Conversion} = \frac{\text{mole of reacted methanol}}{\text{mole of initial methanol}} \times 100 \tag{B-4}$$

$$\% \text{ Yield of Methanol} = \frac{\text{mole of methanol product}}{\text{mole of initial } CO_2} \times 100 \tag{B-5}$$

$$\% \text{ Yield of DME} = \frac{\text{mole of DME product}}{\text{mole of initial methanol}} \times 100 \tag{B-6}$$

$$\% \text{ Yield of Ethylene} = \frac{\text{mole of ethylene product}}{\text{mole of initial ethanol}} \times 100 \tag{B-7}$$

$$\text{Productivity}_j = \frac{\text{mole of desired product } j}{\text{amount of catalyst}} \tag{B-8}$$

B.4 Mole of gas calculation by idea gas law

$$PV = nRT \tag{B-9}$$

P is pressure in bar

V is volume of gas in mL

n is the mole of gas

R is gas constant (83.14 mL·bar·K^{-1}·mol^{-1})

T is temperature in Kelvin

For example, in case of DME synthesis from CO_2 over Cu/ZnO and ferrierite:

Ethanol 100 mL (1.7046 mol) and Cu/ZnO 3 g were loaded into the 250 mL of reactor and then the reactor was pressurized to 36.4 bar by CO_2/H_2 with molar ratio of 1:3 at temperature of 33°C. Mole of initial CO_2 was calculated by Eq. A-1.

$$\text{Mole of initial CO}_2 = \frac{(36.4 \text{ bar}) \cdot (250 - 100 \text{ mL})}{(83.14 \text{ mL bar K}^{-1} \text{ mol}^{-1}) \cdot (273 + 33 \text{ K})} \cdot \frac{1}{4} = 0.0537 \text{ moles}$$

After complete methanol synthesis reaction, the reactor was cooled down to 24°C and 25 bar. There was effluent liquid of 90.5 mL in the reactor. The effluent product was analyzed by a GC equipment as shown in Table B-1 and B-2. The concentration by volume of CO_2, methanol and ethanol were measured by standard calibration curve as shown Figure A-1, A-2 and A-3, respectively. Mole of outlet CO_2 in gas phase and methanol and ethanol in liquid phase was calculated.

Table 16 The effluent product analysis of methanol synthesis in gas phase

No.	Area (Gas phase)				%Volume of CO_2	mole of CO_2
	H_2	N_2	CO	CO_2		
1	11518	9480	7013	45990	8.228	0.0133
2	11875	8552	7222	43058	7.642	0.0123
3	11638	11806	7593	41587	7.347	0.0119
Average	11677	9946	7276	43545	7.739	0.0125

Table 17 The effluent product analysis of methanol synthesis in liquid phase

No.	Area (Liquid phase)			%Volume of MeOH	Mole of MeOH	%Volume of EtOH	Mole of EtOH
	MeOH	EtOH	EtAc				
1	96813	15835852	36419	1.1737	0.0261	87.4831	1.3496
2	103348	17749779	41853	1.2608	0.0280	97.8731	1.5099
3	94906	17166814	41133	1.1483	0.0255	94.7084	1.4610
Average	98356	16917482	39802	1.1943	0.0265	93.3549	1.4402

$$\text{Mole of outlet CO}_2 = \frac{(25 \text{ bar}) \cdot \dfrac{7.739}{100}(250 - 90.5 \text{ mL})}{(83.14 \text{ mL bar K}^{-1} \text{ mol}^{-1}) \cdot (273 + 24 \text{ K})} = 0.0125 \text{ moles}$$

$$\text{Mole of methanol} = \frac{1.1943}{100} \cdot (90.5 \text{ mL}) \cdot \frac{(0.7863 \text{ g mL}^{1})}{(32.04 \text{ g mol}^{1})} = 0.0265 \text{ moles}$$

where density of methanol = 0.7863 g/mL and molecular weight of methanol = 32.04 g/mol

$$\text{Mole of ethanol} = \frac{93.3549}{100} \cdot (90.5 \text{ mL}) \cdot \frac{(0.7853 \text{ g mL}^{-1})}{(46.069 \text{ g mol}^{-1})} = 1.4402 \text{ moles}$$

where density of ethanol = 0.7853 g/mL and molecular weight of ethanol = 46.069 g/mol

The CO_2 conversion and methanol yield were calculated by Eq. B-3 and B-5, respectively.

$$\% \ CO_2 \ \text{Conversion} = \frac{(0.0537 - 0.0125)}{0.0537} \times 100 = 76.7\%$$

$$\% \ \text{Yield of methanol} = \frac{0.0265}{0.0537} \times 100 = 49.4\%$$

80 mL of residue effluent product in liquid phase was loaded in the reactor as the reactant for methanol dehydration to DME, including

$$\text{Methanol} = (0.0265 \text{ moles}) \cdot \frac{80 \text{ mL}}{90.5 \text{ mL}} = 0.0234 \text{ moles}$$

$$\text{Ethanol} = (1.4402 \text{ moles}) \cdot \frac{80 \text{ mL}}{90.5 \text{ mL}} = 1.2731 \text{ moles}$$

After complete reaction, the reactor was cooled down to 22°C and 13.8 bar. The final liquid in the reactor was 72.5 mL. The results which analyzed from GC equipment are shown in Table B-3 and B-4. The concentration by volume of methanol, DME and ethylene were calculated from standard calibration curve as shown in Figure A-2, A-4 and A-5, respectively. Mole of DME and ethylene were calculated.

Table 18 The effluent product analysis of methanol dehydration reaction in gas phase

No.	Area (Gas phase)				%Volume of Ethylene	Mole of Ethylene	%Volume of DME	Mole of DME
	Ethylene	DME	MeOH	EtOH				
1	239309	3530	171845	2066311	1.2995	0.00130	0.1065	0.00011
2	241800	3865	175265	2008120	1.3022	0.00130	0.1072	0.00011
3	246242	4860	176107	1969195	1.3068	0.00131	0.1092	0.00011
Average	242450	4085	174406	2014542	1.3028	0.00130	0.1076	0.00011

Table 19 The effluent product analysis of methanol dehydration reaction in liquid phase

No.	Area (LIQ)					%Volume of Ethylene	Mole of Ethylene	%Volume of DME	Mole of DME
	Ethylene	DME	MeOH	EtOH	EtAc				
1	1740	2372	145943	15656612	37111	1.05043	0.01542	0.10425	0.00121
2	1253	2748	159521	18320566	41812	1.04992	0.01541	0.10499	0.00121
Average	1497	2560	152732	16988589	39462	1.05017	0.01541	0.10462	0.00121

$$\text{Mole of DME (Gas)} = \frac{(13.8\ \text{bar}) \cdot \dfrac{0.1076}{100} (250 - 72.5\ \text{mL})}{(83.14\ \text{mL bar K}^{-1}\ \text{mol}^{-1}) \cdot (273 + 22\ \text{K})} = 0.00011\ \text{moles}$$

$$\text{Mole of DME (Liquid)} = \frac{0.10462}{100} \cdot (72.5\ \text{mL}) \cdot \frac{(0.735\ \text{g mL}^{-1})}{(46.07\ \text{g mol}^{-1})} = 0.00121\ \text{moles}$$

where density of DME = 0.735 g/mL and molecular weight of DME = 46.07 g/mol

Total mole of DME product = 0.00011 + 0.00121 = 0.00132 moles

$$\text{Mole of ethylene (Gas)} = \frac{(13.8\ \text{bar}) \cdot \dfrac{1.3028}{100} (250 - 72.5\ \text{mL})}{(83.14\ \text{mL bar K}^{-1}\ \text{mol}^{-1}) \cdot (273 + 22\ \text{K})} = 0.0013\ \text{moles}$$

$$\text{Mole of ethylene (Liquid)} = \frac{1.05017}{100} \cdot (72.5\ \text{mL}) \cdot \frac{(0.5679\ \text{g mL}^{-1})}{(28.0532\ \text{g mol}^{-1})} = 0.01541\ \text{moles}$$

where density of ethylene = 0.5679 g/mL and molecular weight of ethylene = 28.0532 g/mol

Total mole of ethylene product = 0.0013 + 0.01541 = 0.01671 moles

Finally, the yield of DME and ethylene were calculated by Eq. B-6 and B-7, respectively.

$$\% \text{ Yield of DME} = \frac{0.00132}{0.0234} \times 100 = 5.6\%$$

$$\% \text{ Yield of ethylene} = \frac{0.01541}{1.2731} \times 100 = 1.3\%$$

VITA

NAME	Warangthat Kriprasertkul
DATE OF BIRTH	12 March 1997
PLACE OF BIRTH	Bangkok, Thailand
INSTITUTIONS ATTENDED	Chulalongkorn University, Master of Chemical Engineering, 2019-2021
	Mahidol University, Bachelor of Chemical Engineering, 2015-2019
HOME ADDRESS	100/205 Kanchanapisek Road, Lak Song Sub-district, Bangkae District, Bangkok, Thailand, 10160
PUBLICATION	C. Muangsuwan, W. Kriprasertkul, S. Ratchahat, C.G. Liu, P. Posoknistakul, N. Laosiripojana, C. Sakdaronnarong, Upgrading of Light Bio-oil from Solvothermolysis Liquefaction of an Oil Palm Empty Fruit Bunch in Glycerol by Catalytic Hydrodeoxygenation Using NiMo/Al2O3 or CoMo/Al2O3 Catalysts, ACS Omega, 6 (2021) 2999-3016.

จุฬาลงกรณ์มหาวิทยาลัย
CHULALONGKORN UNIVERSITY

[1] Khunsuphot, สาเหตุภาวะโลกร้อน, Office of the Basic Education Commission, 2010.

[2] N.a.S.I.o. Oceanography, Rise of carbon dioxide unabated, 1315 East-West Highway Silver Spring, MD 20910, 2020.

[3] L. Hancock, Why are glaciers and sea ice melting?, World Wildlife FundWorld Wildlife Fund 1250 24th Street, N.W. Washington, DC 20037, 2020.

[4] C.-H. Huang, C.-S. Tan, A Review: CO_2 Utilization, Aerosol and Air Quality Research, 14 (2014) 480-499.

[5] G. Bonura, C. Cannilla, L. Frusteri, E. Catizzone, S. Todaro, M. Migliori, G. Giordano, F. Frusteri, Interaction effects between CuO-ZnO-ZrO_2 methanol phase and zeolite surface affecting stability of hybrid systems during one-step CO_2 hydrogenation to DME, Catalysis Today, 345 (2020) 175-182.

[6] PubChem, Compound summary of dimethyl ether, National Center fo Biotechnology Information

[7] M. Intelligence, DIMETHYL ETHER MARKET - GROWTH, TRENDS, AND FORECAST (2020 - 2025), India, 2019.

[8] U. Mondal, G.D. Yadav, Perspective of dimethyl ether as fuel: Part I. Catalysis, Journal of CO_2 Utilization, 32 (2019) 299-320.

[9] T. Nakyai, Y. Patcharavorachot, A. Arpornwichanop, D. Saebea, Comparative exergoeconomic analysis of indirect and direct bio-dimethyl ether syntheses based on air-steam biomass gasification with CO_2 utilization, Energy, 209 (2020).

[10] V. L'hospital, L. Angelo, Y. Zimmermann, K. Parkhomenko, A.-C. Roger, Influence of the Zn/Zr ratio in the support of a copper-based catalyst for the synthesis of methanol from CO_2, Catalysis Today, (2020).

[11] J. Xiao, D. Mao, X. Guo, J. Yu, Effect of TiO_2, ZrO_2, and TiO_2–ZrO_2 on the performance of CuO–ZnO catalyst for CO_2 hydrogenation to methanol, Applied Surface Science, 338 (2015) 146-153.

[12] S. Ren, X. Fan, Z. Shang, W.R. Shoemaker, L. Ma, T. Wu, S. Li, N.B. Klinghoffer, M. Yu, X. Liang, Enhanced catalytic performance of Zr modified $CuO/ZnO/Al_2O_3$ catalyst for methanol and DME synthesis via CO_2 hydrogenation, Journal of CO_2 Utilization, 36 (2020) 82-95.

[13] Y. Zhang, D. Li, Y. Zhang, Y. Cao, S. Zhang, K. Wang, F. Ding, J. Wu, V-modified $CuO-ZnO-ZrO_2$/HZSM-5 catalyst for efficient direct synthesis of DME from CO_2 hydrogenation, Catalysis Communications, 55 (2014) 49-52.

[14] Q. Sheng, R.P. Ye, W. Gong, X. Shi, B. Xu, M. Argyle, H. Adidharma, M. Fan, Mechanism and catalytic performance for direct dimethyl ether synthesis by CO_2 hydrogenation over CuZnZr/ferrierite hybrid catalyst, J Environ Sci (China), 92 (2020) 106-117.

[15] F.S. Ramos, A.M.D.d. Farias, L.E.P. Borges, J.L. Monteiro, M.A. Fraga, E.F. Sousa-Aguiar, L.G. Appel, Role of dehydration catalyst acid properties on one-step DME synthesis over physical mixtures, Catalysis Today, 101 (2005) 39-44.

[16] F. Frusteri, M. Migliori, C. Cannilla, L. Frusteri, E. Catizzone, A. Aloise, G. Giordano, G. Bonura, Direct CO_2 -to-DME hydrogenation reaction: New evidences of a superior behaviour of FER-based hybrid systems to obtain high DME yield, Journal of CO_2 Utilization, 18 (2017) 353-361.

[17] N. Tsubaki, M. Ito, K. Fujimoto, A New Method of Low-Temperature Methanol Synthesis, Journal of Catalysis, 197 (2001) 224-227.

[18] S. Likhittaphon, R. Panyadee, W. Fakyam, S. Charojrochkul, T. Sornchamni, N. Laosiripojana, S. Assabumrungrat, P. Kim-Lohsoontorn, Effect of CuO/ZnO catalyst preparation condition on alcohol-assisted methanol synthesis from carbon dioxide and hydrogen, International Journal of Hydrogen Energy, 44 (2019) 20782-20791.

[19] E. Catizzone, A. Aloise, E. Giglio, G. Ferrarelli, M. Bianco, M. Migliori, G. Giordano, MFI vs. FER zeolite during methanol dehydration to dimethyl ether: The crystal size plays a key role, Catalysis Communications, 149 (2021).

[20] G. Bonura, C. Cannilla, L. Frusteri, A. Mezzapica, F. Frusteri, DME production by CO_2 hydrogenation: Key factors affecting the behaviour of CuZnZr/ferrierite catalysts, Catalysis Today, 281 (2017) 337-344.

[21] R. Weingarten, G.A. Tompsett, W.C. Conner, G.W. Huber, Design of solid acid catalysts for aqueous-phase dehydration of carbohydrates: The role of Lewis and Brønsted acid sites, Journal of Catalysis, 279 (2011) 174-182.

[22] C.P. Nash, A. Ramanathan, D.A. Ruddy, M. Behl, E. Gjersing, M. Griffin, H. Zhu, B. Subramaniam, J.A. Schaidle, J.E. Hensley, Mixed alcohol dehydration over Brønsted and Lewis acidic catalysts, Applied Catalysis A: General, 510 (2016) 110-124.

[23] M.A. Armenta, V.M. Maytorena, R. Silva–Rodrigo, L.A. Flores-Sánchez, J.M. Quintana, A. Olivas, Effect of acidity on ferric oxide nanoparticles supported on γ–χ–Al_2O_3 in the methanol dehydration reaction toward dimethyl ether, Fuel, 296 (2021).

[24] E. Hammond, D. Lokhat, Performance comparison of WO_3/SiO_2 to ZSM-5 and γ-Al_2O_3 in the catalytic dehydration of methanol, South African Journal of Chemical Engineering, 36 (2021) 127-133.

[25] M.A. Armenta, V.M. Maytorena, L.A. Flores–Sánchez, J.M. Quintana, R. Valdez, A. Olivas, Dimethyl ether production via methanol dehydration using Fe_3O_4 and CuO over γ–χ–Al_2O_3 nanocatalysts, Fuel, 280 (2020).

[26] X. Dong, F. Li, N. Zhao, Y. Tan, J. Wang, F. Xiao, CO_2 hydrogenation to methanol over Cu/Zn/Al/Zr catalysts prepared by liquid reduction, Chinese Journal of Catalysis, 38 (2017) 717-725.

[27] I. Abbas, H. Kim, C.-H. Shin, S. Yoon, K.-D. Jung, Differences in bifunctionality of ZnO and ZrO_2 in $Cu/ZnO/ZrO_2/Al_2O_3$ catalysts in hydrogenation of carbon oxides for methanol synthesis, Applied Catalysis B: Environmental, 258 (2019).

[28] X. Fang, H. Jia, B. Zhang, Y. Li, Y. Wang, Y. Song, T. Du, L. Liu, A novel in situ grown Cu-ZnO-ZrO_2/HZSM-5 hybrid catalyst for CO_2 hydrogenation to liquid fuels of methanol and DME, Journal of Environmental Chemical Engineering, 9 (2021).

[29] M.M.-J. Li, Z. Zeng, F. Liao, X. Hong, S.C.E. Tsang, Enhanced CO_2 hydrogenation to methanol over CuZn nanoalloy in Ga modified Cu/ZnO catalysts, Journal of Catalysis, 343 (2016) 157-167.

[30] Y. Sun, C. Huang, L. Chen, Y. Zhang, M. Fu, J. Wu, D. Ye, Active site structure study of Cu/Plate ZnO model catalysts for CO_2 hydrogenation to methanol under the real reaction conditions, Journal of CO2 Utilization, 37 (2020) 55-64.

[31] F.C.F. Marcos, L. Lin, L.E. Betancourt, S.D. Senanayake, J.A. Rodriguez, J.M. Assaf, R. Giudici, E.M. Assaf, Insights into the methanol synthesis mechanism via CO_2 hydrogenation over Cu-ZnO-ZrO_2 catalysts: Effects of surfactant/Cu-Zn-Zr molar ratio, Journal of CO_2 Utilization, 41 (2020).

[32] S. Ren, W.R. Shoemaker, X. Wang, Z. Shang, N. Klinghoffer, S. Li, M. Yu, X. He, T.A. White, X. Liang, Highly active and selective Cu-ZnO based catalyst for methanol and dimethyl ether synthesis via CO_2 hydrogenation, Fuel, 239 (2019) 1125-1133.

[33] X. Fang, Y. Men, F. Wu, Q. Zhao, R. Singh, P. Xiao, T. Du, P.A. Webley, Promoting CO_2 hydrogenation to methanol by incorporating adsorbents into catalysts: Effects of hydrotalcite, Chemical Engineering Journal, 378 (2019).

[34] X. A., Methanol Synthesis from CO_2 Hydrogenation with a Cu_Zn_Al_Zr Fibrous Catalyst, Chinese Journal of Chemical Engineering, 17(1) (2009) 88-94.

[35] D. Masih, S. Rohani, J.N. Kondo, T. Tatsumi, Catalytic dehydration of ethanol-to-ethylene over Rho zeolite under mild reaction conditions, Microporous and Mesoporous Materials, 282 (2019) 91-99.

[36] K. Golabek, K.A. Tarach, U. Filek, K. Gora-Marek, Ethylene formation by dehydration of ethanol over medium pore zeolites, Spectrochim Acta A Mol Biomol Spectrosc, 192 (2018) 464-472.

[37] E. Catizzone, M. Migliori, A. Purita, G. Giordano, Ferrierite vs. γ-Al_2O_3: The superiority of zeolites in terms of water-resistance in vapour-phase dehydration of methanol to dimethyl ether, Journal of Energy Chemistry, 30 (2019) 162-169.

[38] A. Aloise, A. Marino, F. Dalena, G. Giorgianni, M. Migliori, L. Frusteri, C. Cannilla, G. Bonura, F. Frusteri, G. Giordano, Desilicated ZSM-5 zeolite: Catalytic performances assessment in methanol to DME dehydration, Microporous and Mesoporous Materials, 302 (2020).